Sep 30th, 2017

B6: Devonian Granite Melt Transfer in Western Maine: Relations Between Deformation, Metamorphism, Melting and Pluton Emplacement at the Migmatite Front

Gary S. Solar
State University of New York College at Buffalo - Buffalo State College, SOLARGS@BUFFALOSTATE.EDU

Paul B. Tomascak
State University of New York at Oswego, tomascak@oswego.edu

Michael Brown
University of Maryland, mbrown@geol.umd.edu

DEVONIAN GRANITE MELT TRANSFER IN WESTERN MAINE: RELATIONS BETWEEN DEFORMATION, METAMORPHISM, MELTING AND PLUTON EMPLACEMENT AT THE MIGMATITE FRONT

By

Gary S. Solar[1], Dept. of Earth Sciences, SUNY College at Buffalo, 1300 Elmwood Avenue, Buffalo, NY 14222
Paul B. Tomascak[2], Dept. of Atmospheric and Geological Sciences, SUNY Oswego, Oswego, NY 13126
Michael Brown[3], Laboratory for Crustal Petrology, Dept. of Geology, Univ. of Maryland, College Park, MD 20742
Email addresses: [1]solargs@buffalostate.edu, [2]tomascak@oswego.edu, [3]mbrown@geol.umd.edu

INTRODUCTION

This trip is designed to examine evidence for syn-tectonic metamorphism, melting and granite magma ascent during transpressive deformation, as recorded by structures, petrology, geochemistry and ages of metasedimentary rocks, migmatites and granites in the Rangeley-Rumford area of western Maine (Figure 1). The trip is intended as a close examination of the variation of mineral fabrics, shapes and sizes of granite bodies (from leucosomes to plutons), and the relation of these to the regional structure, by visiting rocks that were deformed, metamorphosed, and partially melted during the Devonian Acadian orogeny. Data that form the foundation of models developed to explain the evolution of the region are summarized below and are presented by our group in the literature published in the last 20 years (Brown and Solar, 1998a, 1998b, 1999; Brown and Pressley, 1999; Pressley and Brown, 1999; Solar and Brown, 1999, 2000, 2001a, 2001b; Johnson et al., 2003; Tomascak et al., 2005). The field work of Solar (1999) that is the base of these papers owes a debt of gratitude to the career studies of C.V. Guidotti and R.H. Moench, and influence of E-an Zen. The migmatites and the surrounding rocks of this trip are a subset of a 2001 Geological Society of America field excursion (Solar et al., 2001). The rocks of this trip are closely related to non-migmatitic rocks that are the focus of both the 2001 GSA field guide and Trips A2, B1, and B4 of the present NEIGC guidebook. The migmatites are related to the rocks on Trip C6, although our interpretations are dissimilar. The granites on Whitecap Mtn. that are included in part of Trip B5 are part of the granite suite that is a focus of this trip.

The trip is in three parts, corresponding to rock type and timing. The first part consists of Stops 1 and 2 at Coos Canyon and north, the non-migmatitic rocks immediately north of the migmatite front (Figure 2). Rocks at Stops 1 and 2 (and optional stops) illustrate the regional NE-SW-striking structural geology as it is recorded both by folds of the stratigraphic sequence and by the orientation and intensity of metamorphic mineral fabrics. Structural, petrographic, geochemical and geochronological data support the idea that these rocks and structures are characteristic of the migmatite protolith before anatexis. The second part of the trip is devoted to examination of the petrological and structural record of migmatite formation in rocks of the stratigraphic sequence, and the record of granite ascent as illustrated by associated granites in the migmatites (Figure 2; Stops 3 to 8). The third part is the plutons in the system, the Mooselookmeguntic Igneous Complex (MIC) in particular (Figure 2; Stops 9 and 10).

GEOLOGICAL SETTING

The northern Appalachians are divided into NNE-SSW-trending tectonostratigraphic units (Figure 1). The Central Maine belt (CMB), continuous with the Central Mobile belt in Maritime Canada, is the principal unit that occupies most of the eastern part of New England and New Brunswick. The CMB is composed of a Lower Paleozoic sedimentary succession, deformed and metamorphosed at greenschist to upper amphibolite facies conditions, and intruded by plutons of Devonian age (e.g. Moench et al., 1995; Bradley et al., 1998; Solar et al., 1998). The CMB is located between Ordovician rocks of the Bronson Hill belt (BHB) to the W and NW that were deformed and metamorphosed during the Ordovician Taconian orogeny, prior to deposition of the CMB sedimentary sequence. To the SE of the CMB, rocks are Neoproterozoic to Silurian age of the Avalon Composite terrane (ACT).

Regional deformation was partitioned heterogeneously during dextral transpression in response to Early Devonian oblique convergence (van Staal and de Roo, 1995; van Staal et al., 1998). Dextral– SE-side-up

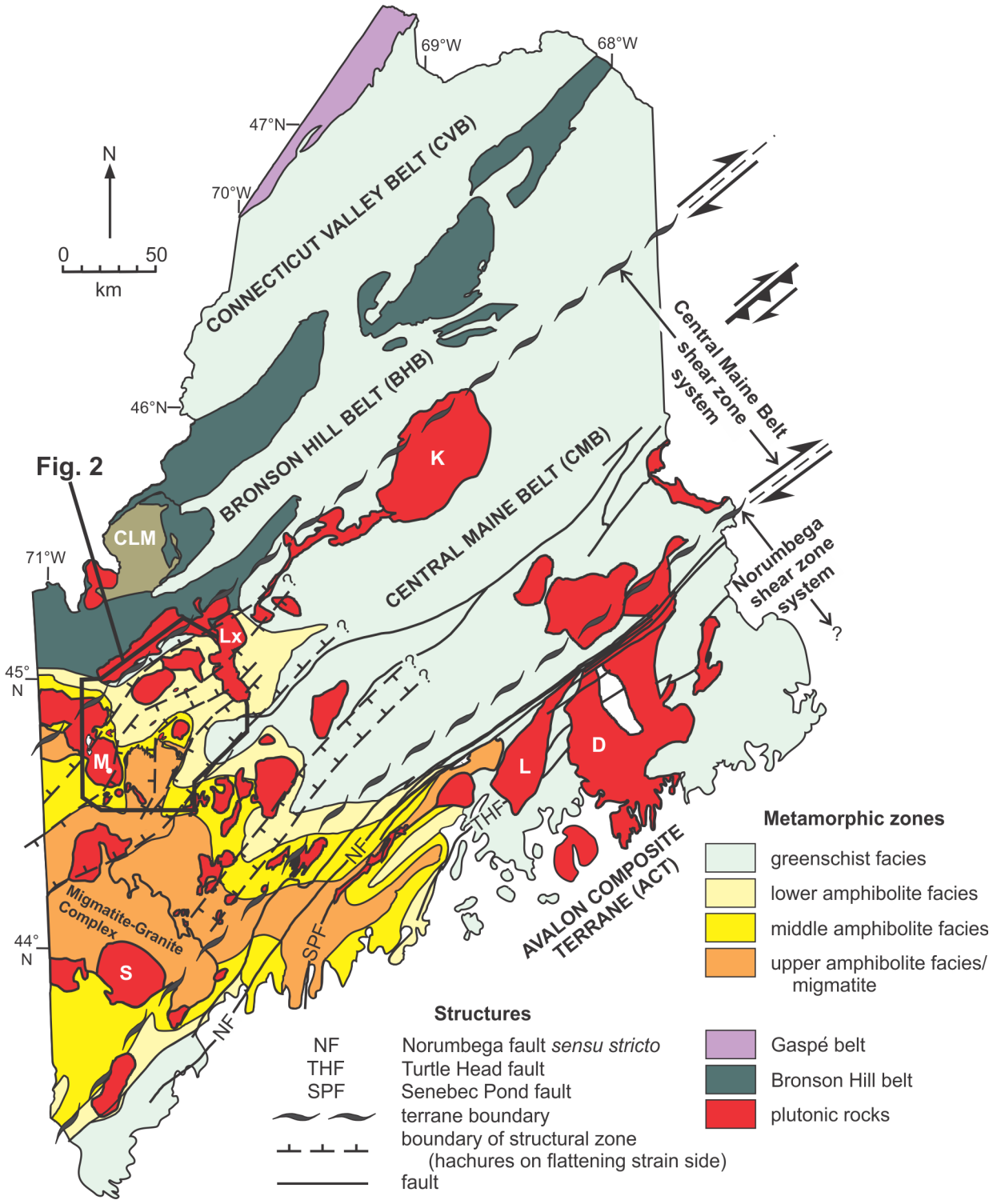

Figure 1. Geological map of Maine illustrating principal tectonic belts, structures, metamorphic zones and plutons (modified after Solar and Brown, 1999; metamorphic zones modified after Guidotti (1989). The Migmatite-Granite Complex and Sebago pluton (S) are subjects of Solar and Tomascak (2016 NEIGC). Pluton distribution is apparently independent of metamorphic zones. Metamorphic zones increase grade NE to SW along regional strike, whereas plutons are apparently arranged into belts that parallel regional strike. Metamorphic isograd patterns are apparently perturbed at structural zone boundaries (Solar and Brown, 2001a). D is Deblois, K is Katahdin, L is Lucerne, Lx is Lexington, M is Mooselookmeguntic, CLB is Chain Lakes Massif.

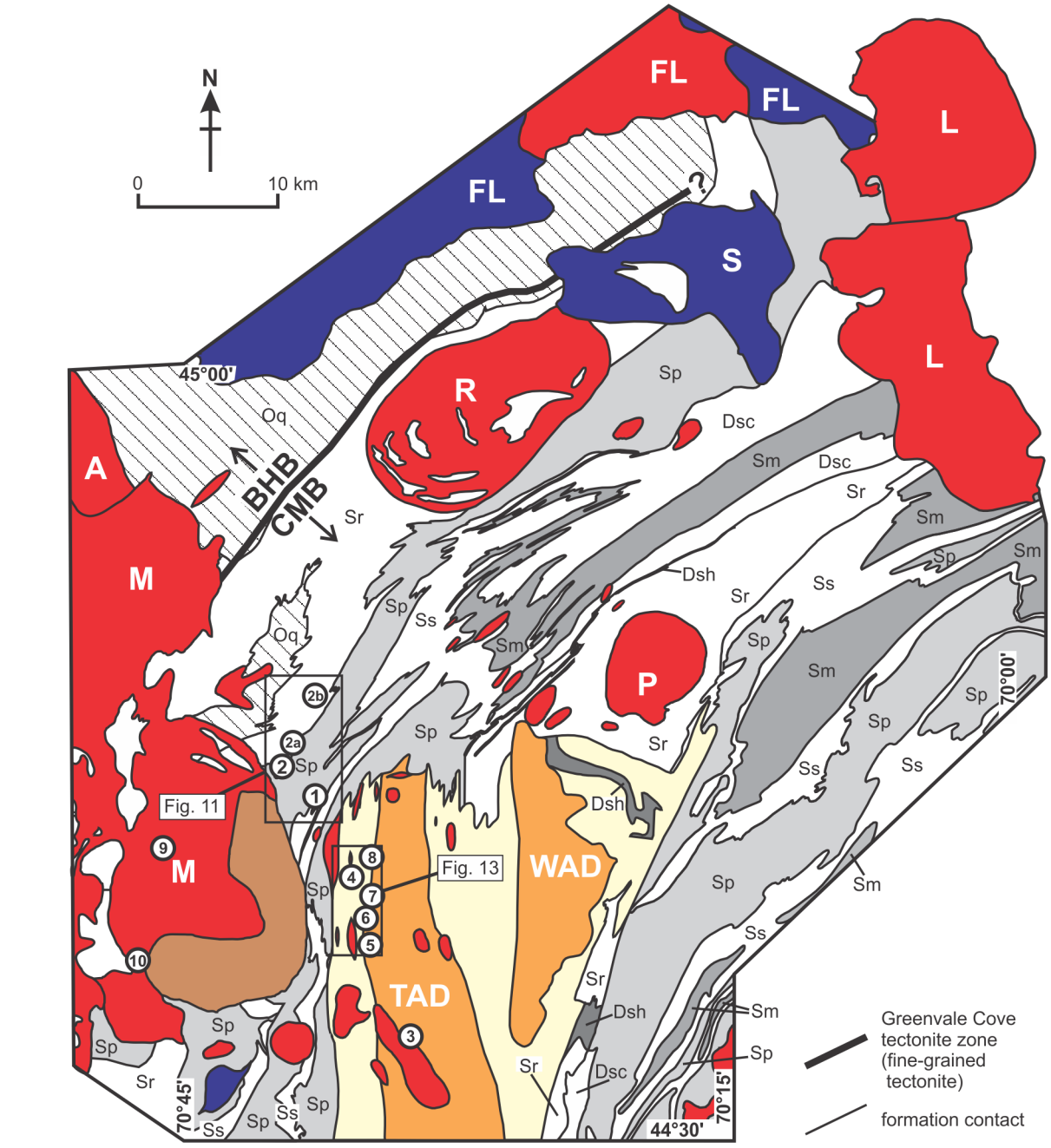

PLUTONIC ROCKS

- A — Adamstown pluton (granodiorite-granite)
- FL — Flagstaff Lake igneous complex (gabbro-diorite/biotite granite)
- L — Lexington pluton (biotite granite-leucogranite)
- M — Mooselookmeguntic Igneous Complex (MIC) (leucogranite/granodiorite)
- P — Phillips pluton (leucogranite, granodiorite)
- R — Redington pluton (biotite granite)
- S — Sugarloaf pluton (gabbro-diorite)
- smaller bodies of plutonic rock

MIGMATITIC ROCKS

- Tumbledown and Weld Anatectic Domains (TAD and WAD; stromatic / heterogeneous migmatite)

METAMORPHIC ROCKS

Central Maine belt
(Rangeley stratigraphic sequence)

Devonian

- Dsh — Hildreths Formation
- Dsc — Carrabassett Formation

Silurian

- Sm — Madrid Formation
- Ss — Smalls Falls Formation
- Sp — Perry Mountain Formation
- Sr — Rangeley Formation

Bronson Hill belt

- Oq — Quimby Formation

③ Field trip stop location and number

Figure. 2. Geological map of the area in western Maine (see Figure 1 for location) (modified after Solar and Brown, 2001a). Within the Rangeley stratigraphic sequence, alternate units are shaded to clarify the map pattern of the stratigraphic succession. Structures in this map area are shown in Figure 3. BHB is Bronson Hill belt and CMB is Central Maine belt. The Greenvale Cove tectonite zone coincides in part with the map pattern of the Greenvale Cove Formation of Moench (1969; 1971) and Moench et al. (1995).

---

displacement was accommodated within the CMB shear zone system (Brown and Solar, 1998a; Solar and Brown, 2001a) while dextral–transcurrent displacement was accommodated within the Norumbega shear zone system (Figure 1; West and Hubbard, 1997; West, 1999) along the southeastern side of the CMB. CMB deformation had ceased by the Carboniferous, and strain localized into the Norumbega shear zone system (West, 1999).

The Rangeley stratigraphic sequence

The CMB is composed of a Silurian to Early Devonian sedimentary succession called the "Rangeley stratigraphic sequence" (Figure 2) that was deformed and metamorphosed during the Devonian (Acadian orogeny; Bradley et al., 1998). The sequence is estimated to be as much as 10 km in thickness, made up of ~5 km each of Silurian and Devonian rocks (Moench and Boudette, 1970). Stratigraphic units are defined in the western Maine area (Figure 2; Moench and Boudette, 1970), and have been extended across most of the New England Appalachians (e.g. Hatch et al., 1983).

The stratigraphy of the sequence is preserved through metamorphism, and begins in the northwest with a proximal coarse conglomerate in the lower part of the Rangeley Formation (Stop 1 of Solar et al., 2001), interpreted to mark the beginning of the Silurian (e.g., Moench, 1970), grades upward (to the SE) into a progressively distal Silurian turbidite sequence and finishes in the central part of the area (Figure 2) with a distal Devonian unit (see Moench et al., 1995, for a complete summary). The sequence has been separated by Moench (1970) into seven apparently conformable formations, based largely on the relative thickness and frequency of alternating centimeter- to decimeter-scale psammite *v.* pelite layers (inferred relict bedding; Moench, 1970; Moench and Boudette, 1970), coupled with variations in the proportion of metamorphic minerals in the pelite layers (R.H. Moench, 1998, personal communication). Locally, cross-stratification is preserved in psammite layers [particularly in the Perry Mountain Formation (STOP 1)]. The summary stratigraphic succession listed in Figure 2 follows the compilation of Moench et al. (1995), modified in the eastern part of the study area after mapping by Solar (1999; Solar and Brown, 2001a).

Regional metamorphism

High-*T* – low-*P* polymetamorphism of the Rangeley stratigraphic sequence in western Maine is well documented, particularly regarding the rocks to the northwest and east of the migmatite domains (Guidotti, 1970, 1974, 1989; Holdaway et al., 1982, 1997; See Figure 2). The trip area is located in the part of Maine where greenschist facies rocks to the northeast increase in grade to upper amphibolite facies within 20 km along strike to the southwest (Figure 3b; see summary in Guidotti, 1989). Across the area, the amphibolite facies rocks are characterized by porphyroblasts of garnet, staurolite and locally pseudomorphed andalusite enclosed within a matrix dominated by muscovite, biotite, quartz, plagioclase, and opaque phases (ilmenite, graphite and pyrite). Fibrolite is an important fabric-forming matrix phase at upper amphibolite facies, especially in migmatitic rocks. The peak of regional metamorphism in western Maine was reached at ca. 404 Ma during the waning stages of transpressional deformation (Solar and Brown, 1999, 2001a, 2001b). Regional isotherms are inferred to have been shallowly inclined at lower grades and closely spaced around synmetamorphic granites and at the migmatite front, consistent with advection-controlled intracrustal redistribution of heat (‘pluton-driven metamorphism’) within the regionally extensive thermal high (Johnson et al., 2003).

Thermodynamic modeling by Johnson et al. (2003) in the MnNCKFMASH subsystem is consistent with field data and implies a metamorphic field gradient from ~3.5-4.0 kbar at lower grades (500-520 °C) to >4.5 kbar at suprasolidus temperatures (> 700 °C). Because peak pressures vary both along and across the strike of the CMB, Brown and Solar (1999) and Johnson et al. (2003) interpreted differential thickening during syntectonic metamorphism. Contact metamorphism associated with the Mooselookmeguntic igneous complex occurred ca. 35 million years after the regional metamorphic peak (Tomascak et al., 2005), and records slightly higher pressure

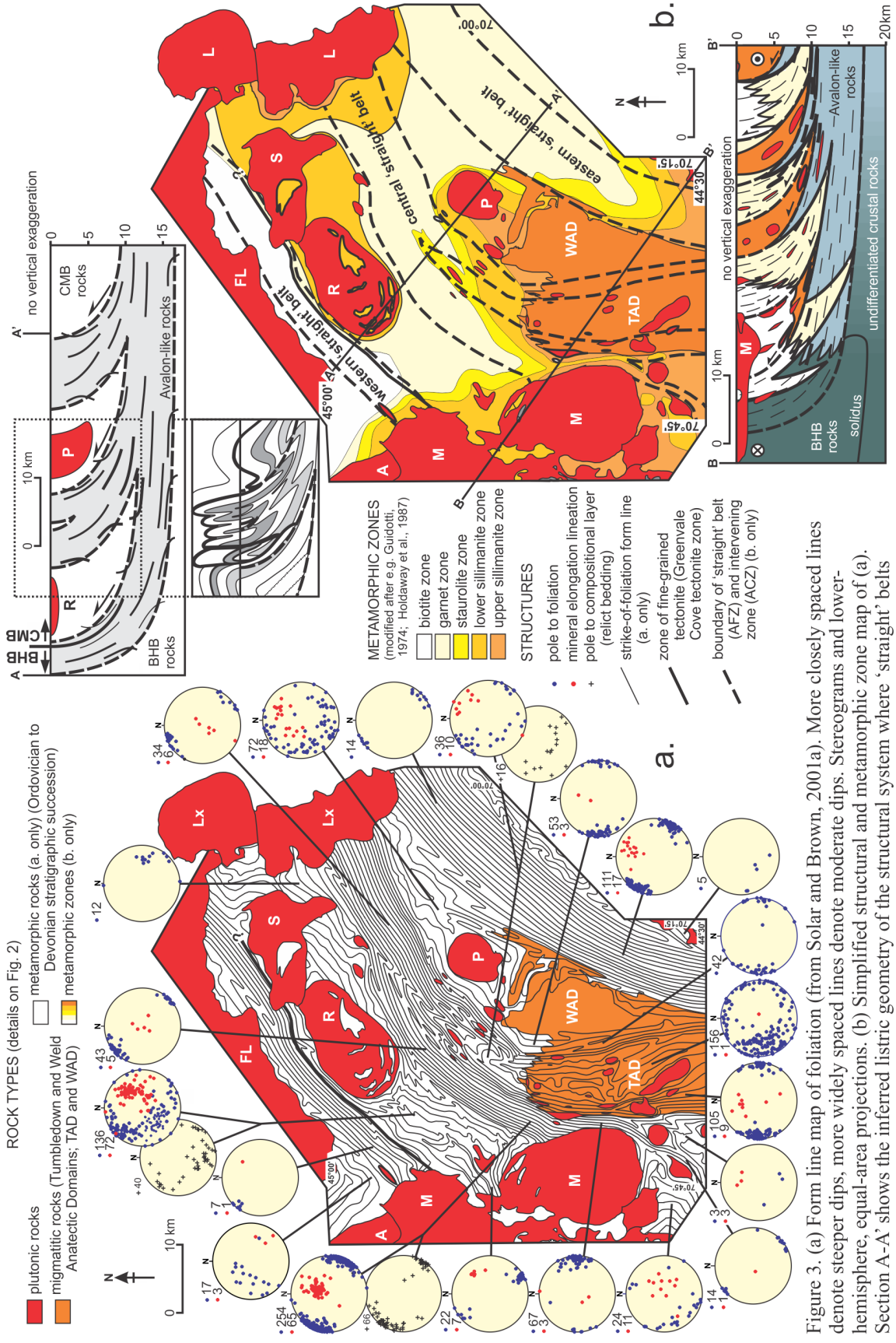

Figure 3. (a) Form line map of foliation (from Solar and Brown, 2001a). More closely spaced lines denote steeper dips, more widely spaced lines denote moderate dips. Stereograms and lower-hemisphere, equal-area projections. (b) Simplified structural and metamorphic zone map of (a). Section A-A' shows the inferred listric geometry of the structural system where 'straight' belts (AFZs; shaded) converge into a root zone at depth (Brown and Solar, 1999). The section below A-A' is the area within the dotted box showing the inferred geometry of folds of the stratigraphic sequence. Section B-B' is drawn to show the higher-grade rocks, particularly the distribution of migmatites. Line segments on both sections are intersections of foliation with the plane of the sections.

conditions than the regional event (Johnson et al., 2005). The final increment of late Acadian thickening beyond ca. 404 Ma accounts for the pressure increase, consistent with the inferred regional cooling prior to the emplacement of the Mooselookmeguntic igneous complex. An overall counter-clockwise *P-T-t* evolution is implied in the CMB (Johnson et al., 2003), consistent with that proposed for Acadian metamorphism in western New Hampshire.

Plutonism

Plutons are kilometer-scale (Figures 1 and 2). In contrast to country rocks, the plutonic rocks record only local evidence of solid-state deformation internally, although foliation is apparently deflected in rocks around the Redington pluton (R; Figures 2 and 3). Some larger-volume plutons cut across the regional structures without either significant deflection of structural trends or formation of a significant deformation aureole (Figure 3a), suggesting displacement of rock out of the map plane. The close association between smaller-volume plutons, such as the Phillips pluton, the Lexington pluton in its northern part, and heterogeneous migmatite in similar structural zones (Figure 3), has been used to suggest a relation between structure, granite ascent and emplacement (Brown and Solar, 1998a, 1998b, 1999; Pressley and Brown, 1999; Solar and Brown, 2001b).

Timing of orogenesis

U-Pb monazite ages from samples of pelite collected from staurolite zone rocks demonstrate two distinct concentrations of metamorphic ages that are interpreted to reflect regional metamorphism at 405-399 ± 2 Ma and contact metamorphism related to the Mooselookmeguntic Igneous Complex (MIC; "M" in Figure 2) at 369-363 ± 2 Ma (Smith and Barreiro, 1990). U-Pb zircon and monazite ages (interpreted to date crystallization) from samples of granite sheets and lenses in stromatic migmatite, and plutons (including the Phillips pluton) are concordant, and are similar in the range ca. 408-404 Ma, except the younger MIC, which yielded ages of ca. 389 and ca. 370 Ma from two discrete granite types (Solar et al., 1998) and younger northern lobe of the Lexington pluton which yielded an age of ca. 365 Ma whereas the central and southern lobes yielded ca. 404 Ma. These data support a model of contemporaneous deformation, metamorphism, and granite ascent (Brown and Solar, 1999).

STRUCTURAL GEOLOGY OF THE RANGELEY-RUMFORD AREA

Two types of structural zone: 'straight' belts and intervening zones

Solar and Brown (2001a) describe the principal structures of western Maine as: (1) the kilometer-scale open to tight folds of the stratigraphic succession, defined by the orientation of centimeter to decimeter scale psammite–pelite compositional layers (see Figure 3b, section A-A'); and, (2) the kilometer scale alternation of structural zones, defined by the NE–SW-striking and steeply SE dipping domainal structure of the CMB shear zone system and the characteristic fabrics of the alternating zones (Figures 1, 2 and 3; Solar and Brown, 1999, 2001a). The regional structure defined by the former is illustrated by the geological map of Fig. 2, whereas the structure defined by the latter is illustrated by the foliation form line map of Figure 3a, in which a pattern emerges of zones of straight and sub-parallel form lines envelope zones where the form lines are more variable in strike. These two types of structural zone coincide with differences in the dip of compositional layers; the layers are more steeply dipping in the zones of straight foliation form lines. The structural style and intensity of fabrics in each of these zones vary with compositional layer and metamorphic grade (Solar and Brown, 1999, 2001a).

Stereograms of the attitudes of mineral fabrics and compositional layers (Figure 3a) show the fundamental difference between each zone. A strong NE-plunging penetrative mineral elongation lineation (amount of plunge variable) is present in metasedimentary rocks in both types of zone, and is defined by the same metamorphic minerals at the same metamorphic grade. In contrast, the intensity and orientation of foliation vary by zone. Where foliation form lines are sub-parallel, foliation is intense and sub-parallel to contacts between compositional layers (Figure 3; see STOP 1). This structural style occurs in 'straight' to arcuate belts at outcrop and map scales (Figure. 3). In contrast, rocks in the intervening zones between these 'straight' belts have conspicuously less intense foliation with variable orientation (Figure 3; see STOPS 2, 2a and 2b). Further, compositional layers in the intervening zones vary in attitude, and are not parallel to foliation in the same outcrop, which transects the layers. At map-scale, the pattern of structural zones shows an alternation of these two types such that 'straight' belts of consistently-oriented NNE-striking planar structures, some of which anastomose, separated by intervening zones, some of which are lens-shaped, in which planar structures vary in orientation (Figure 3). Boundaries between the structural zones are

gradational in outcrop over meter-scale transition zones. Across these transitions, traversing away from 'straight' belts into the intervening zone rocks, compositional layers and foliation is progressively more variable in strike and more moderate in dip, concurrent with lower foliation intensity. However, the orientations of both mineral lineations and hinge lines of folded compositional layers generally do not vary significantly across these transitions. Lineation is equally well developed in both zones, with a progressively more variable attitude across the transition (Figure 3a, stereograms). Contacts between stratigraphic units generally occur within these structural transition zones, as do the transitions between stromatic and heterogeneous migmatite types, but at map-scale unit contacts are transected at a shallow angle by structural zone boundaries (*cf.* Figures 2 and 3). Also, styles of migmatite and shapes of granite bodies within the migmatite domains (TAD and WAD; Brown and Solar, 1999; Solar and Brown, 2001b) vary consistently with structural zone, where stromatic migmatite and sheets of granite are largely within 'straight' belts, whereas heterogeneous migmatite and cylinders of granite occur exclusively within intervening zones (Figure 3).

Structural data collected from 'straight' belt rocks at all grades of metamorphism, including migmatite, show a consistency in orientation of all structural elements that led Solar and Brown (2001a) to suggest nearly complete transposition of compositional layers into sub-parallelism with the tectonic fabric as defined by the matrix minerals. The consistency of orientation of both foliation and lineation across the strike of 'straight' belts suggests that the foliation is sub-parallel to the λ_1-λ_2 plane, and the lineation is sub-parallel to the direction of maximum principal finite stretch (λ_1).

Apparently coeval symmetric structures (e.g. biotite 'fish' and elongate strain shadow tails around porphyroblasts) and en echelon structures [e.g. stacked ramps of compositional layers, tension gashes, ptygmatic folds and shear fractures (all seen at STOPS 1 and 3)] all suggest consistent kinematics: oblique (SE-side-up and dextral) translation (Solar and Brown, 2001a). The obliquity between inclusion trails (S_i) and matrix foliation (S_e), as measured in lineation-parallel thin sections (Figure 4) suggests porphyroblast nucleation and growth occurred before final recrystallization of the matrix minerals (Solar and Brown, 1999, 2001a). Textural zones within porphyroblasts with a successively smaller rake between S_i and S_e suggest progressive rotational reorientation of foliation relative to the porphyroblasts during punctuated porphyroblast growth (Solar and Brown, 2001a). Thus, porphyroblast growth was syn- or inter-kinematic. Solar and Brown (1999, 2001a) proposed that variations in S_i–S_e rake reflect nucleation and growth of porphyroblasts during progressive regional fold tightening of the stratigraphic succession (Figure 5).

Alternating zones of finite strain: AFZs *v.* ACZs

Solar and Brown (2001a) concluded that if the mineral fabrics define the state of finite strain, the ellipsoid defined by grain shapes in the ‘straight’ belts has an oblate to plane-strain shape, consistent with the similarity in orientation between compositional layers and the foliation across the zone. In migmatite in the ‘straight’ belts, the mineral fabrics define a triaxial to uniaxial oblate ellipsoid. Nonetheless, all rocks within 'straight' belts have fabrics that define oblate shapes. Therefore, Solar and Brown (2001a) inferred that 'straight' belts are zones of S > L tectonite where rocks accommodated apparent flattening-to-plane strain, and refer to 'straight' belts as "zones of apparent flattening" (AFZs; Figure 3). The general parallelism of compositional layers and tectonic fabric suggests high strain, consistent with folding and formation of fabrics in response to finite flattening deformation.

In contrast, in rocks of the intervening zones, compositional layers are not rotated into parallelism with the tectonic fabric, but there is a consistency in orientation of all linear structures. This led Solar and Brown (2001a) to interpret a different state of finite strain in these rocks in comparison with rocks in the ‘straight’ belts. The variable orientation and weak definition of the foliation suggests that it did not form parallel to the λ_1-λ_2 principal plane, or that this plane has a variable orientation across zones; however, consistency in orientation of the lineations across the regional strike suggests they formed sub-parallel to the maximum principal finite stretch (λ_1). Structures are symmetrical along the lineation (e.g., strain shadow tails, biotite-quartz pull-aparts along the lineation; STOPS 2, 2a and 2b). This led Solar and Brown (2001a) to suggest dominantly coaxial deformation, with a principal finite stretch along the lineation. As in ‘straight’ belts, fabrics wrap around the porphyroblasts suggesting that nucleation and growth of porphyroblasts to have occurred before final recrystallization of the matrix minerals (Solar and Brown, 1999). Accordingly, Solar and Brown (2001a) concluded that the strain ellipsoid in the intervening zones is a prolate shape, consistent with the well-developed mineral elongation lineation, and the poorly developed foliation that is not consistently parallel to compositional layers. Solar and Brown (2001a) inferred from this that intervening zones are zones of L >> S tectonite, and refer to intervening zones as "zones of apparent constriction" (ACZs; Figure 3b).

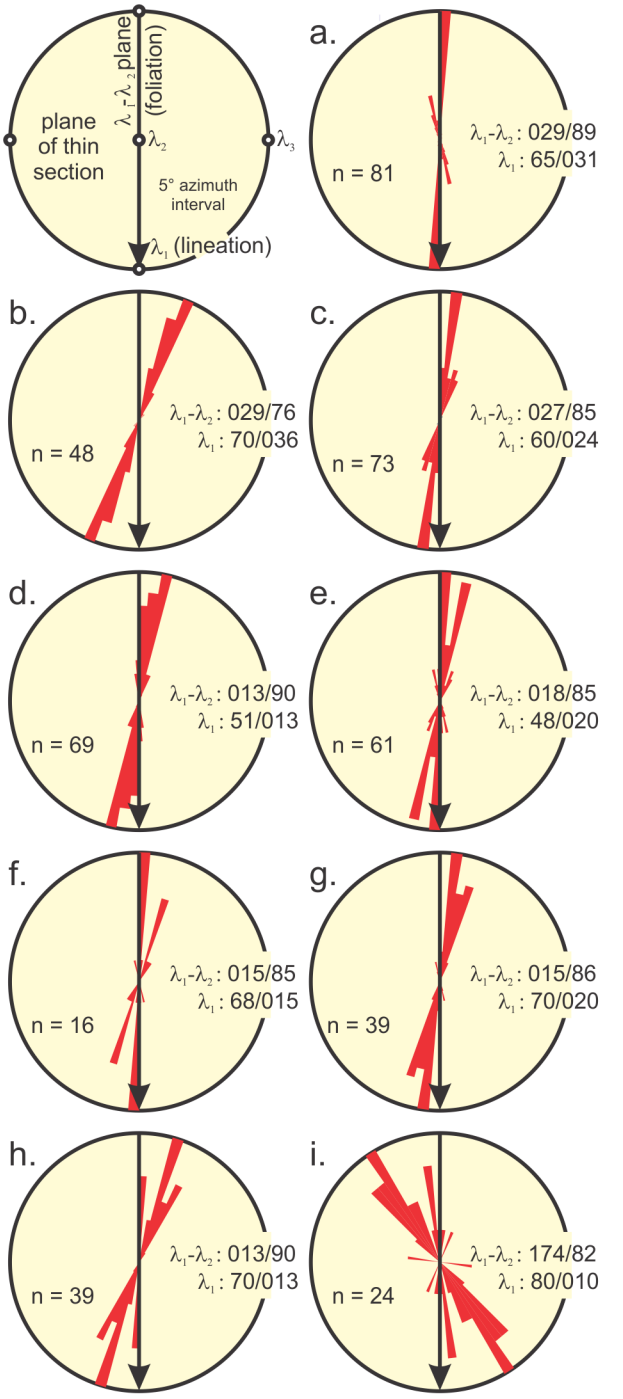

Figure 4. Rose diagrams of Si-Se rakes measured in thin sections cut perpendicular to foliation and parallel to mineral lineation (λ_1–λ_3 plane) from rocks in the central central AFZ, collected at locations across strike (from Solar and Brown, 2001a). d.-h. are from rocks collected at Coos Canyon (STOP 1) at approximately 30 m spacing across strike of compositional layers. The vertical arrow on each diagram shows both the intersection of the foliation with the diagram, and the plunge direction of the lineation in the foliation plane.

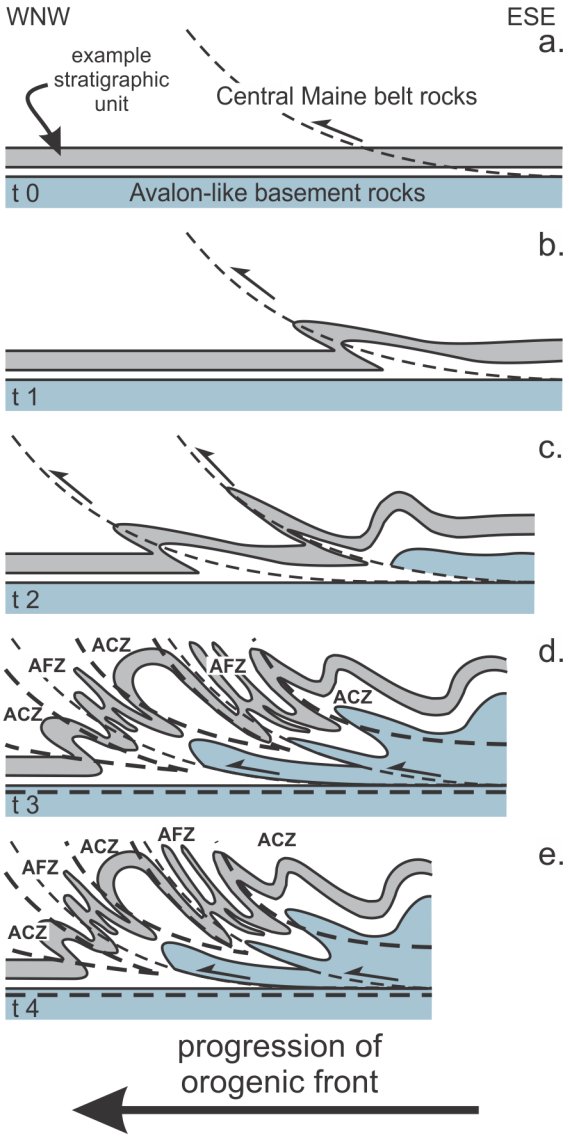

Figure 5. Schematic model sections to show the evolution of the CMB shear zone system in western Maine (from Solar and Brown, 2001a). The shaded fields are the same unit at t0 to t4, and represent the folds of the Rangeley stratigraphic sequence (*cf.* Fig 3b, section A-A') during the development of the structure. At t0 (a), the CMB rocks lay undeformed above basement rocks (stippled field). As the crust shortened, and was contracted inboard (t1, b), the sequence began to buckle asymmetrically to form a ramp-like anticline in the middle crust, detached at the CMB-basement contact. As the system evolved, deformation was localized to tighten folds and strain-harden the sequence (t2, c). Shortening was accommodated progressively more easily, forming zones of flattening strain (AFZs) separated by intervening zones of apparent constrictional strain (ACZs). The alternation between zones corresponds to the areas of tight and open folds, respectively (d and e).

Three-dimensional structure of the CMB shear zone system

Interpretation of the three-dimensional structure of western Maine is based upon the mapped structural pattern and interpretations of various types of geophysical data on the subsurface structure (see Brown and Solar, 1998b, for a discussion). Figure 6 is a lineation-down-NE-plunge perspective block diagram from Solar et al. (1998a) that serves as a summary of the structural system. From the arc described by the 'straight' belts (AFZs) in the map plane (concave to the SE) and their strike length (Figure 3), Solar and Brown (2001a) inferred that the AFZs continue to depth. These zones likely converge into a sub-horizontal root zone at approximately 13 km depth (see Figure 3b, section B-B'). Intervening zones (ACZs) are interpreted to narrow and pinch out with depth. Although ACZs likely thicken upward as the 'straight' belts narrow to maintain strain compatibility, they also change in three-dimensional geometry from lens- shaped to planar, as reflected in the spatial change from SE to NW from deeper to shallower structural levels. Thus, Solar and Brown (2001a) interpreted the three-dimensional shape of the structure to be listric where dips shallow with increasing depth. The steeper plunge of lineations in the central part of the area of Figure 2, where the foliation is rotated from NE- to N-striking (Figure 3a), may reflect deformation in a restraining bend within the structure where steeper lineations may record a larger component of dip-parallel displacement, which may account for the occurrence of migmatite in this area, reflecting exhumation of deeper crust (Figure 6).

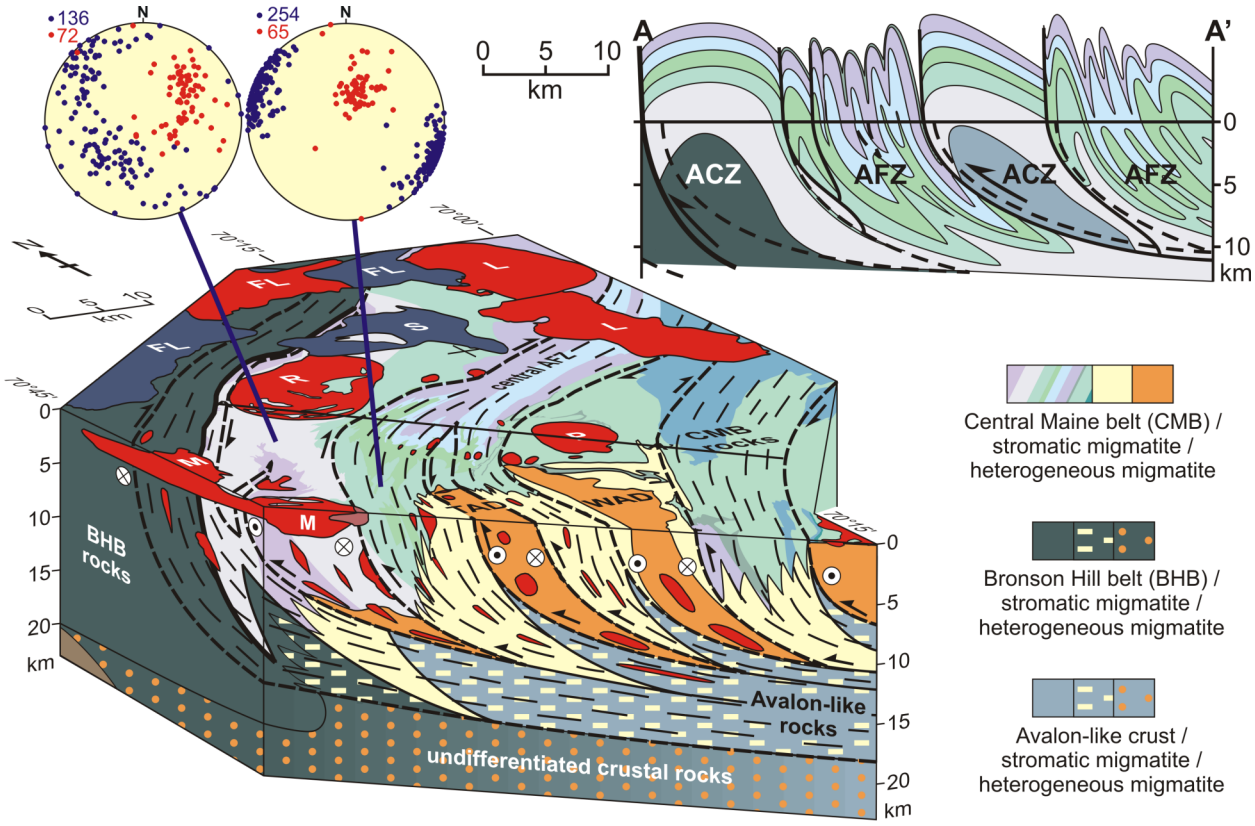

Figure 6. Perspective block diagram of the field area, combining elements of the geological map and sections in Figs. 2 and 3 (after Solar et al., 1998) to show relations between granite plutons and the structural system as described in the text. AFZs are indicated by dashed formlines of fabrics, and ACZs are unornamented. The stratigraphic units are filled with cooler colors whereas the anatectic rocks and basement terranes are ornamented as in Figs. 2 and 3.

MIGMATITE AND GRANITE

The area of excursion is the northern limit of migmatite in the Appalachians, in the Tumbledown and Weld anatectic domains (TAD and WAD, respectively; Figure 2). In western Maine, Solar and Brown (2001b) separate migmatites into stromatic (layered) and heterogeneous (variably-structured) varieties (*cf*. STOPS 4 and 5; see also Brown and Solar, 1999). These two types of migmatite map into discrete zones, with transition zones between, that alternate across the regional strike, roughly corresponding to 'straight' belts (stromatic) and intervening zones (heterogeneous) (Figure 2). Brown and Solar (1999) interpreted both types to have formed at similar structural levels. The structural relations led Brown and Solar (1999) to interpret heterogenous migmatite to be within the cores of regional thermal antiforms (in ACZs; see Figures 2, 3, and 6), flanked by stromatic migmatites (in AFZs). The protolith of the migmatites is interpreted to be rocks of the Rangeley stratigraphic sequence based upon compositional layers that reflect relict bedding, and because the mineral assemblage of sillimanite (fibrolite) + garnet + biotite + quartz + plagioclase + opaque phases ± muscovite ± clinozoisite is consistent with metamorphism of psammite and pelite at upper amphibolite facies conditions (Solar and Brown, 2001b; Johnson et al., 2003). This is supported by the continuation of the regional structure across the migmatite front (Figure. 2, 3, and 6).

Migmatite varies from strongly-foliated metasedimentary rock with a few mm-scale leucosomes per m^2, in which relict primary structures are preserved, to rocks structurally disrupted by the migmatite formation process (progressive metatexis and increasing volume of leucosome, disruption by apparent flow; diatexis) and schlieric granite. Leucosome density and disruption of relict primary structures both increase across strike from the migmatite front (Solar and Brown, 2001b). In both migmatite types, the common matrix hosting the leucosome is sillimanite (mostly fibrolite), biotite, garnet, quartz, plagioclase, opaque phases (usually ilmenite), and coarse, skeletal muscovite books that cut the fabric, interpreted to be retrograde (Solar and Brown, 2001b). Fibrolite and biotite are the main fabric-forming phases, with fibrolite apparently grown at the expense of primary fabric-forming muscovite to suggest it was produced after muscovite breakdown (Solar and Brown, 2001b). Migmatite leucosomes are discrete to diffuse with a common mineralogy of plagioclase, quartz, muscovite, and locally biotite. The microstructure of leucosomes shows crystal faces and mineral films along grain boundaries that suggest some crystallization from melt, and melt-present formation (Solar and Brown, 2001b).

Based on the petrography, Solar and Brown (2001b) interpret the melt-producing reaction as:

$$\text{Ms} + \text{Pl} + \text{Qtz} + \text{water} \rightarrow \text{melt} + \text{Sil} + \text{Bt},$$

followed closely by:

$$\text{Ms} + \text{Pl} + \text{Qtz} \rightarrow \text{melt} + \text{Sil} + \text{Kfs} + \text{Bt},$$

because these two reactions are closely spaced at low *P* (Thompson and Tracy, 1976). At a depth of ~15 km these reactions indicate *T* of > 700°C. Given the limited amount of water-rich metamorphic volatile phases that can be stored in rocks at upper amphibolite facies conditions, melting is dominated by the muscovite-breakdown melting reaction (Johnson et al., 2003). In Maine migmatites, the absence of primary muscovite in migmatites, in comparison with the metasedimentary rocks outside the migmatite front where muscovite averages ~25 vol. % in the mode (Solar and Brown, 2001b), and the universal occurrence of sillimanite as a fabric-forming phase with biotite in the migmatites, suggest that the material that hosts the leucosome is depleted of melt, leading Solar and Brown (2001b) to refer to darker host rock that does not form a distinct melanosome as "melt-depleted host rock". Further, the generally K-feldspar poor nature of leucosomes led Solar and Brown (2001b) to suggest melt has been lost from the migmatites as a whole. These observations are consistent with syntectonic migmatite formation, and consequent syntectonic melt extraction from the anatectic domains. Solar and Brown (2001b) and Johnson et al. (2003) evaluated this postulate in the light of the contemporaneous deformation.

Stromatic-structured metatexite migmatite and associated granites

Approximately half of the exposed migmatite in western Maine is stromatic-structured (layered) metatexite, characterized by a planar structure in which each layer is mineralogically and texturally distinct. This type of migmatite, found mostly in AFZs (Figure 3), is composed of discrete mm- or cm-thick discontinuous sheet-like bodies of granite (leucosome) separated from medium-colored high-grade metamorphic host rock by dark-colored

selvedges (melanosome). The orientation of metatexite layers and mineral fabrics are concordant, as reflected by the consistent steeply dipping orientation of these structures at all scales within each structural zone (Figure 3). At regional scale, the layers are parallel to those of metasedimentary rocks in the same structural zone (Figure 3a, see stereograms).

Leucosomes are trondhjemitic, making up ~3 vol.% of the metatexite at outcrop (Solar, 1999). Millimeter-scale leucosomes range from ~ 1 to 25 cm in length, whereas cm-scale leucosomes are typically ~ 1 to 2 m long; both have low width-to-length ratios. Melanosomes range from 0.1 to 0.6 mm wide, rarely up to 1 mm, and are most conspicuous where in contact with leucosomes. They are composed of > 80 vol.% biotite, accompanied by fibrolite, minor quartz, plagioclase and retrograde chlorite. Biotite, generally ~1 mm long, is clustered with a strongly preferred orientation that defines a foliation parallel to leucosome edges. The intervening host rock layers are 2 to 10 cm thick, being composed of biotite, quartz, sillimanite (mostly fibrolite), garnet, pyrrhotite and/or ilmenite, muscovite (skeletal), and locally plagioclase, tourmaline and clinozoisite. Typically, fibrolite has grown at the expense of primary muscovite in the foliation; the fibrolite forms a fabric in addition to the penetrative biotite foliation, and these sillimanite-biotite folia alternate with quartz-feldspar folia. Fabrics are oriented sub-parallel to fabrics in the metasedimentary rocks outside the migmatite domains down temperature from the migmatite front (Figure 3, see stereograms). Elongate fibrolite aggregates define a steeply plunging lineation visible in the field, and elongate quartz aggregates define a weak sub-horizontal lineation seen in cut hand specimens and suitably oriented thin sections.

Leucosomes show a 3-D 'pinch-and-swell' structure (Solar and Brown, 2001b). A longer wavelength in the sub-horizontal dimension suggests the maximum apparent 'pinch' is sub-vertical and down-dip, consistent with kinematic indicators in the metasedimentary rocks (Solar and Brown, 2001a). This triaxial, oblate shape is similar to that defined by the mineral grains in the host rock layers. Centimeter- to m-scale sub-vertical tabular bodies of granite have cut stromatic-structured migmatite at concordant to weakly discordant angles to the planar structures. Many of these granite sheets are composite (Brown & Solar, 1999), and most have a 'pinch-and-swell' structure with a longer wavelength in the sub-horizontal direction. Within 1 km along strike in the area of STOP 4, a progressive increase occurs in the proportion of m-scale composite granite sheet to host stromatic-structured migmatite such that the metatexite migmatite becomes disrupted (STOP 4) ultimately to occur only as isolated schollen in granites (STOP 4, south part) to make up a sheeted granite complex. Specimens of these granites (from STOP 4 and north) yielded U-Pb zircon ages of 408 ± 2 Ma and 404 ± 2 Ma, respectively (Solar et al., 1998).

Heterogeneous metatexite and associated granites

A regular planar structure is absent in the remainder of the exposed migmatite in western Maine, an observation that led Solar and Brown (2001b) to refer to these migmatites as "heterogeneous", found exclusively in ACZs. The orientation of grain-shape fabrics and geometry of leucosomes vary more in these rocks than in the stromatic-structured metatexite migmatite (Figure 3a, see stereograms). Weak foliations and lineations in heterogeneous migmatite are defined by sillimanite (mostly fibrolite) and biotite. There are two types of heterogeneous migmatite, vein-structured metatexite migmatite in the S and SW and diatexite migmatite in the N and NE. Contacts between the two types are gradational over tens of meters in transition zones (Solar and Brown, 2001b). Simply, vein-structured metatexite migmatite (STOP 3) has phlebitic, or veined leucosomes, and this type typically displays meter-scale compositional layers interpreted to be relict from the protolith (Solar and Brown, 2001b). Diatexite migmatite (STOPS 5, 6 and 7), in contrast, is a rock in which the protolith structures are not observed, suggesting destruction by diatexis. Vein-structured metatexite migmatite shows sharp leucosome contacts. In contrast, contacts between leucocratic and melanocratic domains in diatexite migmatite are diffuse and gradational at the cm-scale.

Vein stromatic-structured metatexite migmatite. Centimeter-scale pod- or lens-shaped trondhjemitic leucosomes up to 20 cm long are separated by cm-scale anastomosing darker host layers similar to the melanosomes of stromatic-structured metatexite migmatite. Leucosomes make up ~15 vol.% on outcrop surfaces, and display 'pinch-and-swell' structure (Solar and Brown, 2001b). The melanosomic host rock contains sillimanite (mostly fibrolite), biotite, muscovite, plagioclase, quartz, pyrrhotite and/or ilmenite, garnet and locally K-feldspar. Sillimanite is found as clots within both muscovite and plagioclase. Biotite (1-3 mm in length), muscovite, and elongate untwinned plagioclase (up to 6 mm long) all show a distinct grain shape fabric, defining a strong moderately dipping foliation (variable dip direction) and weak, moderately-plunging, down-dip lineation.

Diatexite migmatite. Diatexite migmatite varies at outcrop from 'patchy' leucosome-dominated to biotite-sillimanite-dominated rock, and outcrop to outcrop from schlieren-rich diatexite migmatite to schlieric granite with schollen of vein-structured migmatite and non-migmatitic calc-silicate-rich psammite (Solar and Brown, 2001b). Most types are characterized by a discontinuous, weakly-defined foliation of variable attitude. Leucosomes and leucocratic domains make up ~9 to 15% of diatexite migmatite outcrop surfaces, and are generally uniformly distributed. Discrete leucosomes appear as cm-scale quartzo-feldspathic mineral domains that vary from diffuse to sharp at their margins, and have sub-equant shapes in pavement outcrops, 1 to 2 cm in diameter, but are elongate down-dip of the sillimanite fabric in the host rock, with lengths up to 20 cm (Solar and Brown, 2001b; see STOP 5). Thus leucosomes tend to be rod-shaped, plunging moderately-to-steeply ENE, sub-parallel to both the weakly-defined mineral lineation in the host rock and the strongly-defined mineral lineation in the metasedimentary rocks outside the migmatite front (Solar and Brown, 2001b). These fabrics define a triaxial, strongly prolate shape similar to that of the metasedimentary rocks in the same structural zones (ACZs; Figure 3).

Diffuse domains of the host rock interfinger with the leucosome at the mm-scale, and consist of biotite, sillimanite (mostly fibrolite) and garnet, with accessory muscovite, plagioclase, quartz, pyrrhotite and/or ilmenite, and K-feldspar (Solar and Brown, 2001b). Fibrolite has grown at the expense of muscovite and untwinned plagioclase to form a younger generation of foliation-forming minerals. Different proportions of these minerals account for the gradual variation of diatexite migmatite from more quartzo-feldspathic (leucocratic) to more ferro-magnesian (melanocratic) types (Solar and Brown, 2001b), both seen at STOP 7. In the extreme case, either schlieric granite is formed (leucocratic diatexite migmatite; STOP 8), or the mineral assemblage is dominated by biotite, sillimanite and garnet with less than 10 vol.% (plagioclase and quartz) to give the rock a melanocratic appearance (STOP 7). Biotite, muscovite and elongate untwinned plagioclase show a preferred grain-shape fabric that defines a weak, moderately-to-steeply dipping foliation and strong, moderately ENE-plunging, down-dip lineation.

Most outcrops of diatexite migmatite are cut by meter-scale, cylindrical granite bodies (STOP 7). These granite bodies are elongate subparallel to the mineral lineation in diatexite migmatite, and to the rod-shaped leucosomes (see Brown and Solar, 1999, for a discussion). Entrained blocks of strongly foliated biotite-garnet schist are found in the interior of the granite cylinders. The granite cylinders lack a fabric, except proximal to the margin of these blocks. An example of the granite cylinders (from STOP 7) yielded an age of ca. 400 Ma (Solar, Brown and Tucker, unpublished data).

The Phillips pluton

Immediately NE of the WAD (Figure 2) is the coeval Phillips pluton (ca. 404 Ma; Pressley and Brown, 1999), that is interpreted to be hemi-ellipsoidal with long dimension parallel to the regional moderately NE-plunging lineation (Brown & Solar, 1998b; 1999; Pressley & Brown, 1999). It is located in an ACZ, similar to the diatexite migmatites, and it has a similar geometry to the smaller-volume cylinders of granite found in heterogeneous migmatites (STOP 7). These observations have been used to suggest a relationship between structure, granite ascent and emplacement (Brown and Solar, 1999). The geochemistry of common leucogranite (~95% by area) from the Phillips pluton has been interpreted to reflect an origin by melting after muscovite dehydration of a source with geochemical characteristics similar to the metasedimentary rocks of the CMB (Pressley and Brown, 1999). The remaining ~5% by area is granodiorite interpreted to reflect an origin by melting after biotite dehydration in a source geochemically similar to "Avalon-like" rocks (Figure 7a; see Fig. 1). The bodies of granite found in the migmatites do not possess this latter component (Figure 7a). For these reasons, Solar and Brown (2001b) evaluated what relation exists between the migmatites, the smaller-volume granites in the migmatites and the common leucogranite of the Phillips pluton.

The Mooselookmeguntic Igneous Complex (MIC)

The MIC was previously mapped as three petrographically distinct plutonic bodies: the Mooselookmeguntic, Umbagog and Adamstown plutons (Figure 2; Moench et al., 1995). Considering new data, Tomascak et al. (2005) grouped the MIC into two principal types of rock: biotite granodiorite to quartz monzodiorite (the monzodiorite suite), and biotite and two-mica granite to granodiorite (granite). Biotite monzodiorite to granodiorite enclaves, petrographically similar to rocks of the monzodiorite suite, occur in the granite. The monzodiorite suite dominates the southwestern portion of the complex (previously the Umbagog pluton). The enclaves in the MIC granite occur as multi-meter-scale blocks with petrographic character similar to the monzodiorite suite. Portions of both the

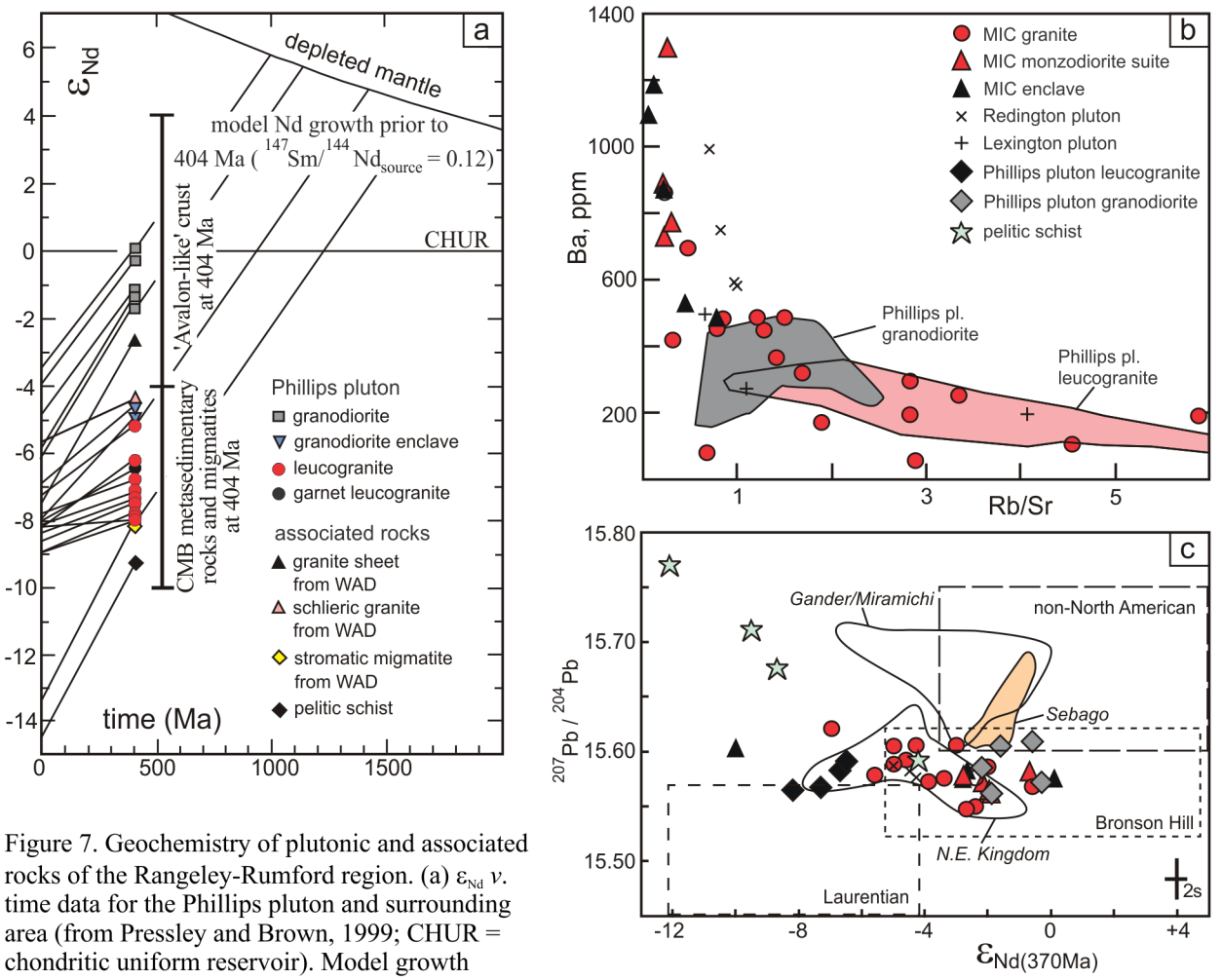

Figure 7. Geochemistry of plutonic and associated rocks of the Rangeley-Rumford region. (a) ε_{Nd} *v.* time data for the Phillips pluton and surrounding area (from Pressley and Brown, 1999; CHUR = chondritic uniform reservoir). Model growth trajectories before 404 Ma are calculated using a crustal value of 0.12 for $^{147}Sm/^{144}Nd$ (ave. shale compositions). The range of ε_{Nd} (at 404 Ma) in the two most likely sources are shown for reference. (b) Rb/Sr *v.* Ba concentration for rocks of the Mooselookmeguntic Igneous Complex (MIC), the Phillips pluton and other regional plutons (from Tomascak et al., 2005). See Fig. 2 for locations of these bodies. Fields for the Phillips pluton from Pressley and Brown (1999). The MIC granite (open circles), the Phillips pluton and the Lexington pluton have low Ba concentrations and Rb/Sr ratios significantly greater than unity. The Redington pluton and the MIC granodiorite and enclave are distinctly high in Ba concentration, and consistently low in Rb/Sr ratio. (c) ε_{Nd} *v.* $^{207}Pb/^{204}Pb$ for plutonic rocks and associated pelitic schist (after Tomascak et al., 2005). Symbols list is in b. Pelitic schist (open stars) from Ayuso and Schulz (2003) and Arth and Ayuso (1997). White fields with italic labels define ranges of paired Nd, Pb data for northern Appalachians granites (Siluro-Devonian Gander zone and Ordovician Miramichi highlands plutons from New Brunswick: Whalen et al., 1996, 1998; Northeast Kingdom batholith, Vermont, granites: Arth and Ayuso, 1997). Dashed rectangular fields show estimated ranges for basement terranes based on unpaired Nd, Pb data from the literature (see Tomascak et al., 2005, for a discussion).

---

monzodiorite suite and the granite lie to the north and south of the BHB-CMB contact (Figure 2). The Adamstown pluton in the north ("A" in Figures.2 and 3) is split from the MIC based upon penetrative solid-state fabrics not found in the rest of the body. Solar et al. (1998) reported crystallization ages for two MIC rocks: a U-Pb zircon age of 389±2 Ma for a granodiorite enclave (referred to as "biotite granite"), and a concordant U-Pb monazite age of 370±1 Ma for a granite ("two-mica leucogranite"). Tomascak et al. (2005) reports two samples from distinct parts of the MIC monzodiorite suite yield identical ages, slightly older than the granite (one is at STOP 10, see Figure 2 for

location; ca. 377 Ma on four concordant to 3% discordant U-Pb zircon fractions). This is equivalent to the U-Pb concordia upper intercept age of 378±2 Ma published by Moench and Aleinikoff (2002) for an alkali gabbro "border facies" of the monzodiorite suite.

Other plutonic rocks

The Redington pluton in the CMB is dominantly a porphyritic biotite granite that has its northern boundary coincident with the tectonite zone that separates the BHB and CMB (Figure 2). Tomascak et al. (2005) report the upper U/Pb intercept age of four zircon fractions is 408±5 Ma (from Solar et al., 1998), and two concordant zircon fractions that suggest an age of ca. 406 Ma is more accurate. The Sugarloaf pluton (2 specimens; Figure 2; Tomascak et al., 2005) occupies a similar position to the Redington pluton, but is apparently mingled felsic-mafic rocks that bear strong resemblance to large portions of the more mafic part of the adjacent Flagstaff Lake intrusive complex. Rocks are dominantly gabbroic with subordinate felsic rock pods. The Lexington composite pluton comprises northern, central and southern portions, based partly on interpretation of the 3-dimensional character of the pluton (Brown and Solar, 1998b, 1999), occurring east along strike from the main body of the MIC (Figure 2). Rock types are primarily granite and granodiorite, based on normative composition, with gabbro enclaves. All granite samples contain biotite and some contain two igneous micas. One U-Pb zircon age determined by Solar et al. (1998; 404±2 Ma) is from the central portion of the Lexington pluton, and an identical concordant zircon age from the southern lobe is reported by Tomascak et al. (2005; ca. 403 Ma). Tomascak et al. (2005) also report a younger age from the northern lobe (ca. 365 Ma, two concordant U-Pb zircon fractions).

GEOCHEMISTRY

Major- and trace-element and isotope geochemistry of the granitic rocks is summarized in Figures 7 and 8, and in Pressley and Brown (1999; Figure 7a), Solar and Brown (2001b) and Tomascak et al. (2005; Figures 7b and 7c). See Brown and Solar (2001b) and Johnson et al. (2003) for summaries of the geochemistry of the migmatites and surrounding metasedimentary rocks (Figure 8). In regard to the migmatite geochemistry (Figure 8), textures show that biotite was apparently stable on a regional basis, indicating that the biotite dehydration melting reaction was not crossed during regional metamorphism. Solar and Brown (2001b) constrained the processes involved in leucosome and pluton formation by comparing whole-rock and migmatite component geochemistry versus experimental melt and residuum compositions (Figure 8). Based on the structural evolution of western Maine (Solar and Brown, 2001a), and the field relations and geochemistry of the metatextite and diatexite migmatites, and granites (Figure 8), Solar and Brown (2001b) proposed a model of progressive separation of melt and residue during deformation of the CMB metasedimentary succession. Based upon field relations and geochemistry (Figure 8), metasedimentary rocks similar in composition to those of the CMB are inferred to be the protolith for the migmatites. The depleted nature of metatexite and diatexite migmatites is not balanced by the smaller-volume granites alone (Figure 8). The Harker plots in Figure 8 (a. to d.), and the K_2O *v.* Na_2O plot (Figure 8e) indicate that differential separation of melt from residual solid material was not the sole petrogenetic process involved in producing the variation observed. If mass balance is preserved at all scales during melting, melt segregation and transfer, and crystallization of the melt, then the processes involved may be tracked in the ternary plot K – (Fe* + Mg + Ti) – (Na + Ca) (Figure 7f). In such a plot, biotite lies along the edge (Fe* + Mg + Ti) – K; it represents the major residual phase. The feldspar join is represented by the edge (Na +Ca) – K, close to which lie melts produced from crustal protoliths. Residual compositions will be displaced from the field of metasedimentary rocks toward (Fe* + Mg + Ti) – K, whereas leucosome and granite compositions will trend toward the feldspar join. In Figure 8f, migmatite compositions are displaced toward the (Fe* + Mg + Ti) – K edge in comparison with the CMB metasedimentary rock field, whereas granites and leucosomes are weakly clustered toward the feldspar join, closer to the (Na + Ca) apex than the K apex. The three specimens from the block of biotite-garnet schist (from STOP 7) plot between biotite and plagioclase, but much closer to biotite, and are displaced from the CMB metasedimentary rock field toward garnet, reflecting the dominance of these phases in the rock (Solar and Brown, 2001b). The whole rock chemistry of the schlieric granite specimen of STOP 8 plots between the field of CMB metasedimentary rocks and the feldspar join, suggesting the specimen is enriched in the feldspathic components compared to the protolith composition. The migmatite leucosomes are seen to define an array of compositions from melt-dominated, plotting close to the MBS melt compositions in the experiments, to cumulate-dominated, plotting close to a cumulate composed of ~80% plagioclase and ~20% biotite. Variable loss of a K-rich liquid is implied (Solar and Brown, 2001b). In contrast, the smaller-volume granites define a triangular field between the MBS melts and the cumulate join between plagioclase and biotite, with the leucosome array as the bottom edge and extending along the cumulate join from ~20 to ~35%

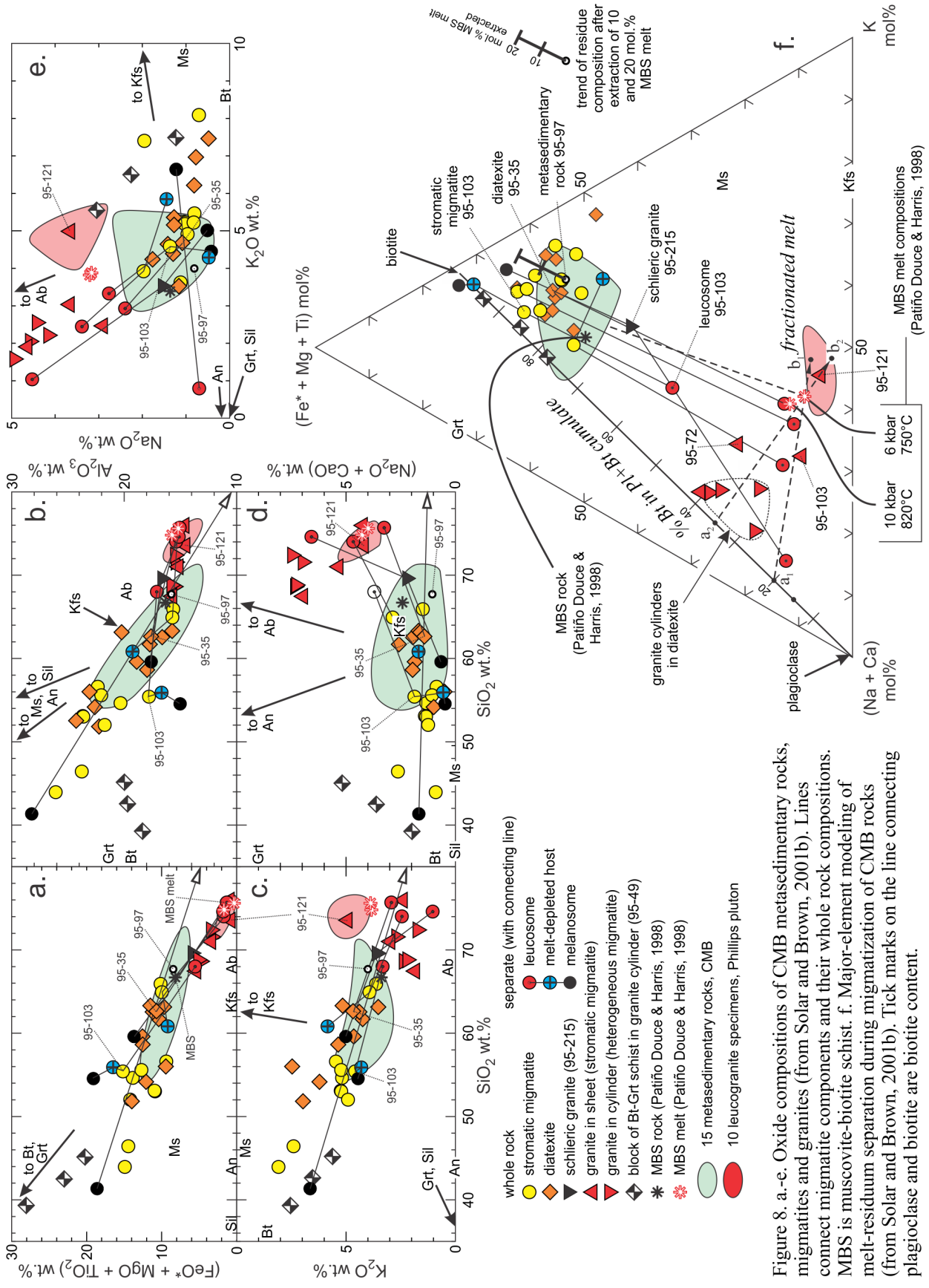

Figure 8. a.-e. Oxide compositions of CMB metasedimentary rocks, migmatites and granites (from Solar and Brown, 2001b). Lines connect migmatite components and their whole rock compositions. MBS is muscovite-biotite schist. f. Major-element modeling of melt-residuum separation during migmatization of CMB rocks (from Solar and Brown, 2001b). Tick marks on the line connecting plagioclase and biotite are biotite content.

biotite. The common leucogranite of the Phillips pluton and one other granite specimen crystallized from a K-enriched (evolved) liquid in comparison with the MBS melts. Based on data in Figure 8f, Solar and Brown (2001b) inferred that none of the smaller-volume granites has a melt composition, but instead they have cumulate compositions, each with a variable amount of cumulate material and residual, fractionated liquid, possibly with some residual biotite and plagioclase; a K-rich liquid has been partially lost from these rocks.

Rare earth elements. Assuming the CMB metasedimentary rocks were the protolith for the TAD and WAD migmatites, and the source for the granites, Solar and Brown (2001b) normalized to REE contents to one representative metasedimentary rock (Figure 9; see Solar and Brown, 2001b, for discussion). Examination of the protolith normalized REE patterns shows that whole rock compositions of the migmatites resemble the protolith closely, but are generally enriched in total REE, likely reflecting melt loss at the scale of the hand specimen relative to the protolith. All granites have REE patterns that lie well below the protolith composition, and all but granite 95-121 have positive Eu anomalies. One granite specimen from the diatexite shows LREE-enrichment relative to the protolith. The melt-depleted host rock in the migmatites is REE-enriched, with the exception of one specimen that shows MREE depletion. Leucosomes show variable total REE depletion. Schlieric granites are slightly depleted in the REE, although 95-215 (STOP 8) shows slight HREE enrichment. Consistent with the cumulate hypothesis, migmatite leucosomes and smaller-volume granite commonly exhibit positive Eu anomalies. The common leucogranites from the Phillips pluton are REE depleted in a similar fashion to the smaller-volume granites, and are closely similar to the pattern of granite 95-121. Complementing the suite of granites, the three analyses from the

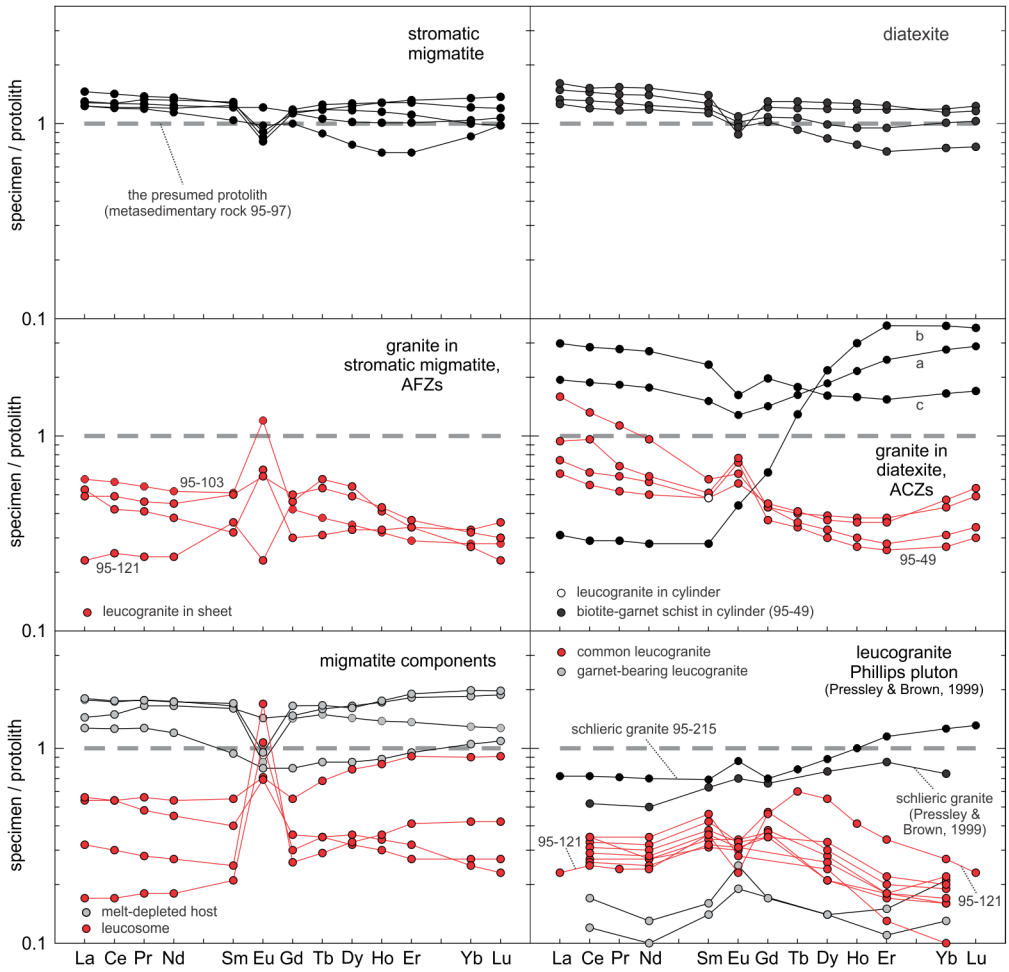

Figure 9. REE concentrations of leucogranite, migmatite and migmatite components normalized to a representative metasedimentary rock (represented by the heavy dashed line) (Fig. 12 in Solar and Brown, 2001b).

block of biotite-garnet schist (from STOP 7) show strong total REE enrichment, with the exception of the LREE of one specimen (b) that may reflect the higher proportion of garnet in that specimen (Solar and Brown, 2001b).

DISCUSSION: TRANSPRESSIVE DEFORMATION AND GRANITE ASCENT

Solar and Brown (2001a) interpreted the CMB shear zone system to have developed as a thrust system during dextral-transpressive deformation in response to Early Devonian (Acadian) oblique convergence (Figure. 5 and 6). The deformation was partitioned between zones of apparent flattening strain (AFZs, the 'straight' belts) and zones of apparent constrictional strain (ACZs, the intervening zones). This partitioning was a consequence of the serial development and subsequent progressive modification of thrust ramps in the Silurian to Early Devonian stratigraphic succession above the Avalon-like basement (Figure 3b, section B-B'), a model that is consistent with the tectonic model for the Acadian orogeny of Bradley et al. (1998), which primarily uses the crystallization age of plutons to suggest that the Acadian orogenic front migrated inboard during the Devonian. A relative increase in volume in the ACZs as the AFZs encroached on them with progressive accommodation of strain is suggested as a mechanism to maintain the prolate fabrics (Solar and Brown, 2001a). The model is consistent with models of transpression zones, where strain is distributed heterogeneously into belts of contrasting finite deformation (Robin and Cruden, 1994), and in which the transpression zone is stretched along strike (Dias and Ribeiro, 1994).

Regarding the relation of melt flow in this structural system, Solar and Brown (2001b) noted that melt loss from metatexite and diatexite migmatites is implied by the K-feldspar poor nature of the leucosomes, an idea that is supported by the residual chemistry of the host rock, and the lack of mass balance of trace elements between migmatite components to suggest open-system behavior at the scale of hand specimens. The 'pinch and swell' structure of granite sheets (e.g., at STOP 4) is consistent with melt flow during deformation and weak strain during or after emplacement. The strong correlation of regional fabrics across the migmatite front (field 'solidus') in the same structural zone (Figure 3a) supports the interpretation that migmatite formation occurred while the rocks were accommodating strain. Solar and Brown (2001b) postulated that leucosomes and smaller-volume granites record evidence of syntectonic melt flow within and through the migmatite, and that granite in plutons apparently outside the migmatites at the level exposed represent evolved melt that escaped syntectonically from a similar source to the migmatites exposed currently in the TAD and WAD.

Given the steep fabric orientation, Solar and Brown (2001b) interpreted the retrograde muscovite and chlorite to be a consequence of buoyancy-aided fluid flow parallel to the rock fabrics. This fluid is likely to have been derived from crystallizing melts in the migmatites (Figure 10). As melt crystallizes in the deforming rocks, liberated H_2O

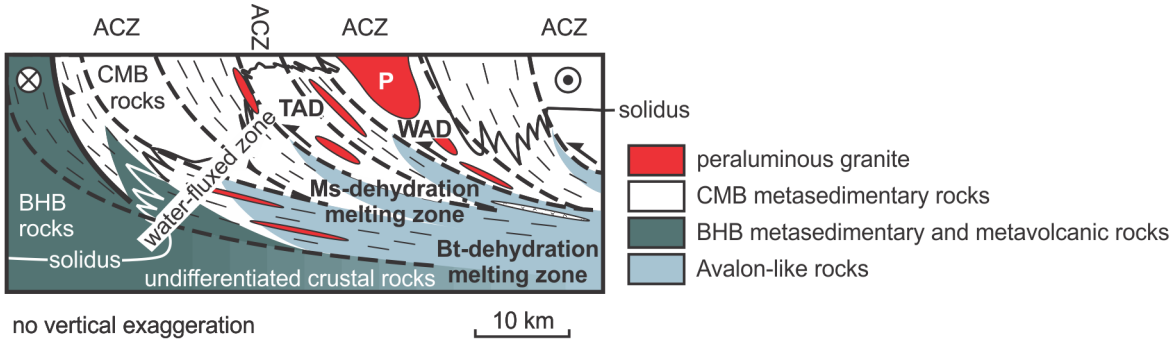

Figure 10. Schematic structure section of an orogenic system based upon the Maine example (after Brown and Solar, 1999; Fig. 14 in Solar and Brown, 2001b). The section is sub-vertical along the line A-A' in Fig. 2b. The "solidus" corresponds to the migmatite front, the margin of the anatectic domains TAD and WAD (Fig. 2). Heavy dashed lines are the boundaries of structural domains (Figs. 1 and 2). Solar and Brown (2001b) use this diagram to explain that the migmatite front, which tracks the solidus, was progressively extended into shallower parts of the orogenic system by advection of material during contractional thickening. Granite, traveled via this syntectonic system, crystallize at the solidus and exsolves a water-rich volatile phase that we postulate was responsible for widespread generation of retrograde muscovite in migmatites and retrogression of staurolite and andalusite in subsolidus rock (Solar and Brown, 2001b).

may promote melting in adjacent units at suprasolidus conditions or retrogression at subsolidus conditions. No influx of water-rich volatile phase is necessarily implied or required. Solar and Brown (2001b) postulated this is the principal cause of regional syntectonic retrogression of staurolite and andalusite in rocks outside the migmatite front.

SUMMARY AND CONCLUDING STATEMENT

In Maine, metamorphism and granite crystallization are contemporaneous; and syntectonic magma ascent was controlled by deformation and development of strain fabrics. Mineral assemblages and geochemical data are consistent with melting after muscovite-dehydration reactions, and suggest that migmatite leucosomes and smaller volume granites represent cumulate rocks (+/- residual material and some retained fractionated melt) that complement common leucogranite in the Phillips pluton. Metatexite and diatexite migmatite residual geochemistry relative to the metasedimentary rocks, and the 'pinch and swell' structure of granite sheets, are consistent with melt loss from those rocks, perhaps driven by the accommodation of deformation. Schlieric granites suggest some melt redistribution prior to melt loss, in this case leaving a more felsic cumulate than the residual migmatites.

Migmatites preserve evidence in cumulate leucosomes of the flow network that drained these rocks of an evolved melt. We postulate that migmatites similar to those exposed represent the source of common leucogranite in the Phillips pluton. Thus, the Phillips pluton may be connected at depth to granites similar to those found in the migmatites of the TAD and WAD, in the manner described by Brown and Solar (1999) where the heterogeneous migmatites and granites in ACZs formed in the cores of thermal antiforms developed during regional contraction (Figures 2, 3, 6 and 10). However, the relation between migmatite leucosomes, smaller-volume granites and leucogranite in plutons is not straightforward and involves multiple processes. It is naïve to expect that migmatite leucosomes and leucogranite in plutons should show simple melt compositions without entrained residue or modification by fractional crystallization. This is likely given the common association of migmatite leucosomes and smaller-volume granites with cumulate compositions, whereas the leucogranite of adjacent plutons is consistent with the putative liquid lost from these rocks. The classically popular notion that migmatites represent 'failed' granites has been reconsidered in the light of multiple syntectonic processes (see Sawyer, 2008, and references therein).

ROAD LOG

Mileage

0.0 Begin at the Coos Canyon Rest Area parking lot at the intersection of Maine Rt. 17 and Weld Rd. in the town of Byron adjacent to the Coos Canyon Campground, ~ 6 miles north of Roxbury, Maine.

STOP 1: PERRY MOUNTAIN FORMATION (SP), COOS CANYON, BYRON, MAINE

(UTM 4842161N, 368525W)

See Figure 11 for location. Plastically deformed meta-turbidite (Silurian; centimeter-scale alternating layers of pelite and psammite) similar to that at STOPS 2 and 3. Layers and mica foliation are both steeply ESE-dipping. There is a moderately to steeply NNE-plunging penetrative bladed muscovite and acicular biotite lineation. Fabrics are viewed best using mutually perpendicular outcrop surfaces. Pelite layers are staurolite bearing throughout, locally andalusite bearing (pseudomorphs), and show distinct centimeter-scale 'P'- and 'Q'-domains defined by matrix minerals (Solar and Brown, 2001a). The long-axis orientations of staurolite porphyroblasts were measured at two locations here, and those data are discussed in Solar and Brown (1999; see their Figures 4b and 4c).

This outcrop is within the central zone of apparent flattening strain (Brown and Solar, 1999; Solar and Brown, 2001a). Because of the extent of this outcrop, most structures common to rock within the zones of apparent flattening strain are found here, including the restricted variation of foliation and lineation attitudes (see Figure 3). Other structures include meter-scale domains of meter-scale tight folds of the compositional layers with transecting foliation. Biotite fish are apparent locally along surfaces eroded sub-parallel to the mica lineations. Brittle structures are also present including left-stepping en echelon quartz-filled gashes (restricted to the psammite layers), and dextrally offset quartz-filled shear fractures with larger apparent offset in the pelite layers. Foliation-parallel surfaces are best to view the apparent preferred fabrics, including the apparent alignment of staurolite and andalusite. Staurolite is replaced within meter-

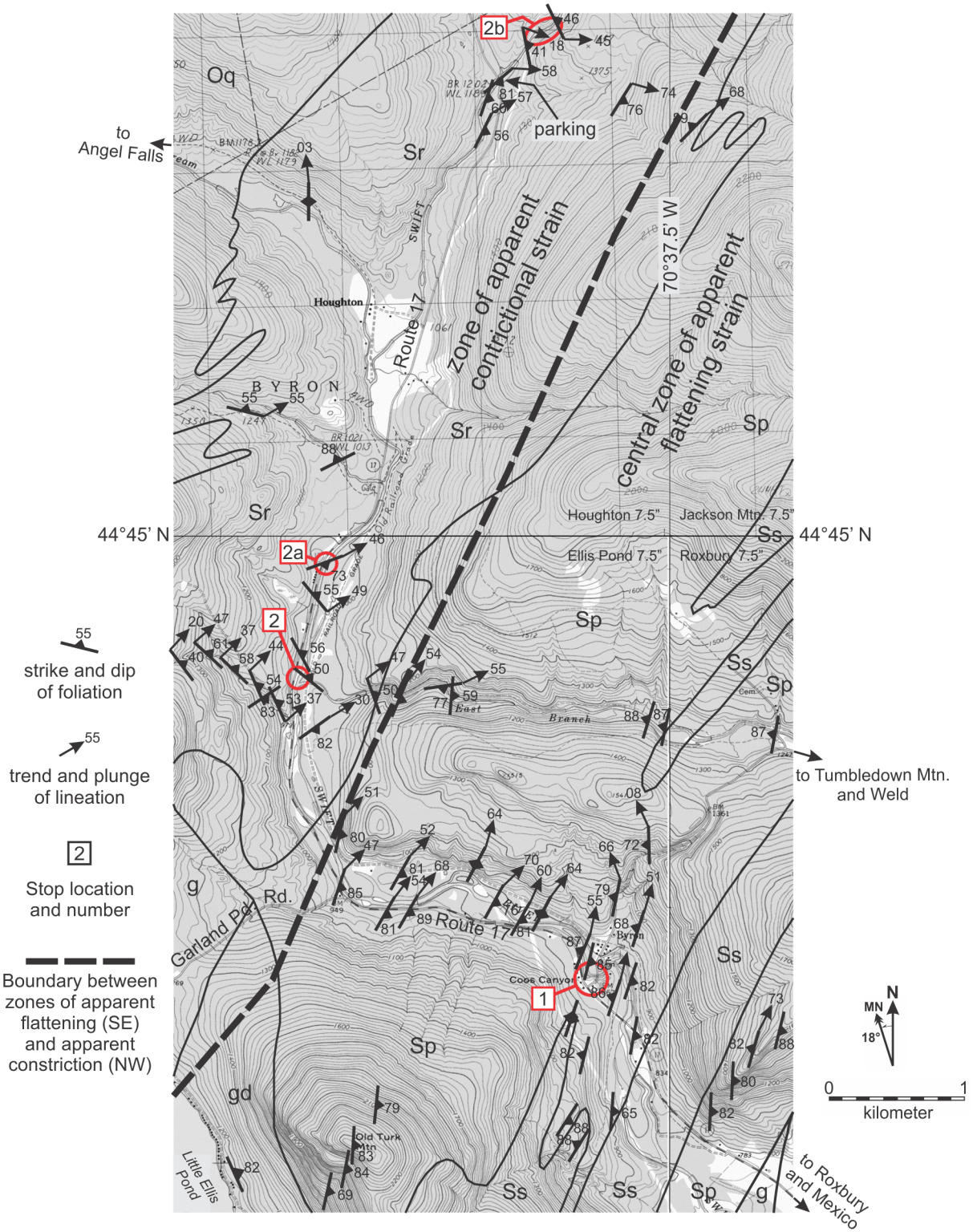

Figure 11. Topographic, simplified geologic and location map for the area of STOPS 1 and 2, and optional stops 2a and 2b. Structural data are taken from Solar (1999). Symbols are consistent with those on Fig. 2; Oq is Quimby Formation, Sr is Rangeley Formation, Sp is Perry Mountain Formation, Ss is Smalls Falls Formation. g is granite and gd is granodiorite of the Mooselookmeguntic pluton in the SW. The location of Maine Rt. 17 is highlighted across the map (along Swift River. See road log for details of STOP locations and geology).

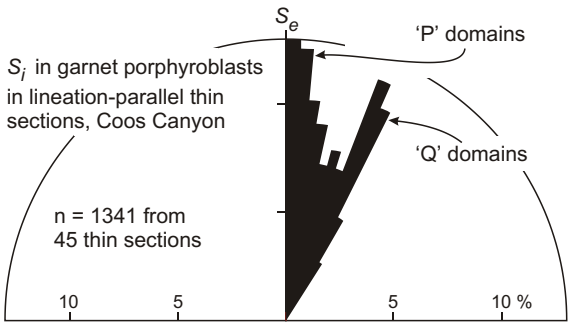

Figure 12. S_i-S_e for garnet from a 133 m traverse of Coos Canyon (after Steely, 2001). The plane of the diagram is parallel to the thin sections, all perpendicular to foliation, the interection of which is the vertical line. The bimodal distribution defines two distinct populations of garnet relative to 'P' domains and 'Q' domains. The different populations suggest differences in the competency between the two matrix domains (Steely, 2001).

scale domains across strike at this location. Some andalusite has pink cores remaining after partial replacement.

Three of the Rose diagrams in Figure 4 (d, f and h; from Solar and Brown, 2001a) are S*i*-S*e* rakes illustrated by porphyroblasts in rocks at this locality. Rakes were measured for each porphyroblast in the three thin sections cut from rocks collected across strike. These data show a distinct and consistent obliquity, the breadth of which Solar (1999) attributed to the diachronous growth histories of the main porphyroblasts, garnet vs. staurolite, garnet having more strongly discordant inclusion trails relative to the matrix foliations in all thin section views. Solar and Brown (2001a) interpreted these data to reflect a record of punctuated (inter-kinematic) porphyroblast growth during progressive deformation/reorientation and recrystallization of matrix fabrics. Steely (2001) confirmed a difference in obliquities between porphyroblast phases, but also found a difference between porphyroblasts located in 'P'- and 'Q'-domains (Figure 12), and between porphyroblasts viewed in lineation-parallel vs. lineation perpendicular thin sections.

Mileage

0.0 Turn right to go north on Rt. 17.
1.2 Intersection of Rt. 17 and Garland Pond Road (road to Little Ellis Pond; Figure 11).
2.0 Dirt access road on left along West Branch of Swift River.
2.3 Park on right side of road at the turnout where the Swift River is joined by the East Branch of Swift River (Figure 11). The outcrop for STOP 2 is in the Swift River, west bank, accessed via the path to the river.

STOP 2: RANGELEY FORMATION (SR), SWIFT RIVER, UPSTREAM FROM (NORTH OF) COOS CANYON, BYRON, MAINE (UTM 4955439N, 368599W)

See Figure 11 for location. Plastically deformed meta-turbidite (Silurian; centimeter-scale alternating layers of pelite and psammite) similar to that at STOP 1 with the notable exception that the variation of compositional layer attitudes is large, not 'straight' by comparison with layers at Coos Canyon (see Figure 3). This STOP, along with Optional Stops 2a and 2b (Figure 11), are listed here to demonstrate the structural variation of the intervening zones between zones of apparent flattening (e.g., STOP 1; Coos Canyon is an extensive outcrop, but STOPS 2 and 2a are only small exposures). Compositional layers are in open folds that penetrate the outcrop. Layers and mica foliation are not sub-parallel, and foliation here is only weakly developed (*cf.* STOP 1). However, as at Coos Canyon, there is a moderately NNE-plunging penetrative bladed muscovite lineation, but unlike at Coos Canyon, there is a biotite-pull-apart lineation that is parallel to the muscovite lineation. Pelite layers are staurolite-bearing (partially replaced). These fabrics illustrate the apparent constriction recorded here, and in the intervening zone in general (i.e. zone of apparent constrictional strain). This rock is just NW of the central zone of apparent flattening strain (Brown and Solar, 1999; Solar and Brown, 2001a), within the zone of apparent constriction, but is transitional to the two structural zones in that foliation is better developed here relative to typical rocks in the zones of apparent constrictional strain (just north, see Figure 11 for example optional stops 2a and 2b).

---------- Optional Stops 2a and 2b ----------

** STOPS 2a and 2b are other examples of rocks similar to those at STOP 2, typical of rocks in the intervening zone to the west of the central 'straight' belt (Figures 2 and 3). These stops have their own road log starting at STOP 2. Return to STOP 2 to resume the trip road log.

Optional stop mileage

0.0 Continue north on Rt. 17.
0.6 Park on side of Rt. 17 just north of three houses located on the left (west) side of the road (Figure 11). The outcrop for STOP 2a is pavement in the Swift River, upstream of the houses.

STOP 2a (*optional*): RANGELEY FORMATION (SR), SWIFT RIVER, HOUGHTON, MAINE
(UTM 4956299N, 368836N)

See Figure 11 for location. Plastically deformed meta-turbidite (Silurian; centimeter-scale alternating layers of pelite and psammite) similar to that at STOP 2. Note the mesoscopic biotite-quartz pull-aparts with long dimension parallel to the muscovite elongation lineation (moderately NNE-plunging). Compositional layers define an open fold, and mineral lineations are sub-parallel to the fold hinge line, but are more steeply NNE-plunging. Again, foliation here is only weakly developed (*cf.* STOP 1).

Optional stop mileage

0.6 Continue north on Rt. 17.
1.0 Bridge over West Branch Swift River (Figure 11).
1.3 Bridge over Swift River (Figure 11).
1.8 Intersection with road to Angel Falls (on left; Figure 11). Continue north on Rt. 17.
3.0 Park in dirt lot on the east side of the road just before (south of) the bridge over Swift River (Figure 11). Walk upstream (east, right) through the woods via the dirt road, and along the path to the powerline. Continue on the path across the powerline, and decend along the path afterward, down to the river for STOP 2b.

STOP 2b (*optional*): RANGELEY FORMATION (SR), SWIFT RIVER GORGE, HOUGHTON, MAINE
(UTM 4960186N, 370476W)

See Figure 11 for location. Plastically deformed meta-turbidite (Silurian; centimeter-scale alternating layers of pelite and psammite) similar to that at STOPS 2 and 2a. Compositional layers are variable in moderately NE dip. Pelite layers are staurolite bearing throughout, and the replacement of the staurolite is also extensive. Note the "new" staurolite growth within the staurolite pseudomorphs. This "new" growth is due to thermal aureole effects of the nearby Mooselookmeguntic pluton (west of this location; Figures 2 and 11, and STOPS 9 and 10). The long-axis orientations of the pseudomorphs were measured here, and those data are discussed in Solar and Brown (1999; see their Figure 4h).

---------- End of Optional Stops ----------

Road log continues from STOP 2.

Mileage

2.3 Turn around and return south on Rt. 17.
4.6 Coos Canyon.
7.8 Meter-scale sheets of biotite granite along east bank of the Swift River.
8.7 Roxbury town center.
9.3 Outcrops of diatexite migmatite in Swift River (STOP 7).
9.5 Intersection with Walker Brook Road on left (to STOP 8).

10.9 Outcrops of diatexite migmatite in Swift River (STOP 6).
12.0 Outcrops of diatexite migmatite in Swift River (STOP 5).
12.3 Intersection with Rt. 120 access road at Frye, ME (the road to STOPS 4, 9 and 10).
13.7 Roadcuts of diatexite migmatite.
14.8 Black Bridge Road. (Outcrops in the Swift River under the bridge are stromatic-structured metatexite migmatite.)
15.8 Turn right into "Mexico Recreation Park" and continue through the park, past the athletic fields to the parking area at the far northwest end (close to the Swift River which flows along the west end of the park). The outcrops for STOP 3 are in the river as pavement exposures.

STOP 3: VEIN MIGMATITE (HETEROGENEOUS MIGMATITE), SWIFT RIVER, MEXICO, MAINE
(UTM 4937207N, 375839W)

Pod-shaped (vein) leucosomes in a stromatic-structured meteatexite migmatite that is plastically deformed. We interpret this as the former metasedimentary rock similar to that of STOPS 1 and 2. This exposure is large enough to see the similarities between this rock and the non-migmatite stratigraphic sequence (the centimeter-scale alternating layers of pelite and psammite in the Perry Mountain Formation, at Coos Canyon; STOP 1). Vein leucosomes and melt-depleted host rock (interpretation based on geochemical data discussed in Solar and Brown, 2001b) are restricted to the meta-pelite layers, except where they are discordant to layers and formed within right-stepping en echelon shear fractures across the foliation, and where they define left-stepping en echelon ptygmatic folds, also across the foliation (both suggest right-lateral shear along the compositional layers). Compositional layers and foliation are sub-parallel and dip moderately ENE. Foliation in the meta-pelite domain is defined by penetrative fibrous sillimanite and biotite. This rock is within the domain of heterogeneous migmatites in the southern part of the TAD (Figure 2). Structurally, this rock is typical of vein-structured metatexite migmatite within the intervening zone between the western and eastern limbs of the central zone of apparent flattening, but is located near the transition zone between the heterogeneous and stromatic-structured migmatite (see STOP 4) (Solar and Brown, 2001a, 2001b). This outcrop is used by Solar and Brown (2001b) as evidence that the Silurian metasedimentary rocks are the protolith for the migmatites because of the structural and geochemical similarities between the rock types.

Mileage

15.8 Return to Rt. 17.
16.3 Left turn on Rt. 17 to return north to Roxbury.
17.8 Pass intersection with Black Bridge Road on left. Continue north on Rt. 17.
20.4 Turn left on access road to Rt. 120 in Roxbury (Frye).
20.5 Bridge over Swift River.
20.6 Turn right onto dirt logging road that goes north into the woods (on left side of a house). This logging road is visible on the satellite photograph in Figure 13. Pass the driveway for the house. This is an active logging road. Limit your speed to 25 mph, and yield to logging vehicles.
20.7 Pass through logging road gate and continue north on the logging road as it follows Swift River upstream.
22.3 Left-hand curve in road (away from Swift River at STOP 6; Figure 13).
22.4 Bridge over Philbrick Brook (Figure 13).
22.9 Bridge #2.
23.1 Pass intersection with dirt road to left (Figure 13). Continue straight.
23.3 Bridge #3.
23.5 Powerline (Figure 13).
24.3 Bear left and intersection with road to Bunker Pond (Figure 13).
24.9 Bridge #4.
25.3 Bridge #5.
25.5 Bridge #6
25.6 Bear right to go east on main logging road (Figure 13), and cross the powerline for a second time (Fig. 13).
26.1 Turn right onto dirt logging road (Figure 13) and cross over bridge immediately.
26.4 Continue straight onto narrower logging road (do not turn left to go down to the river).

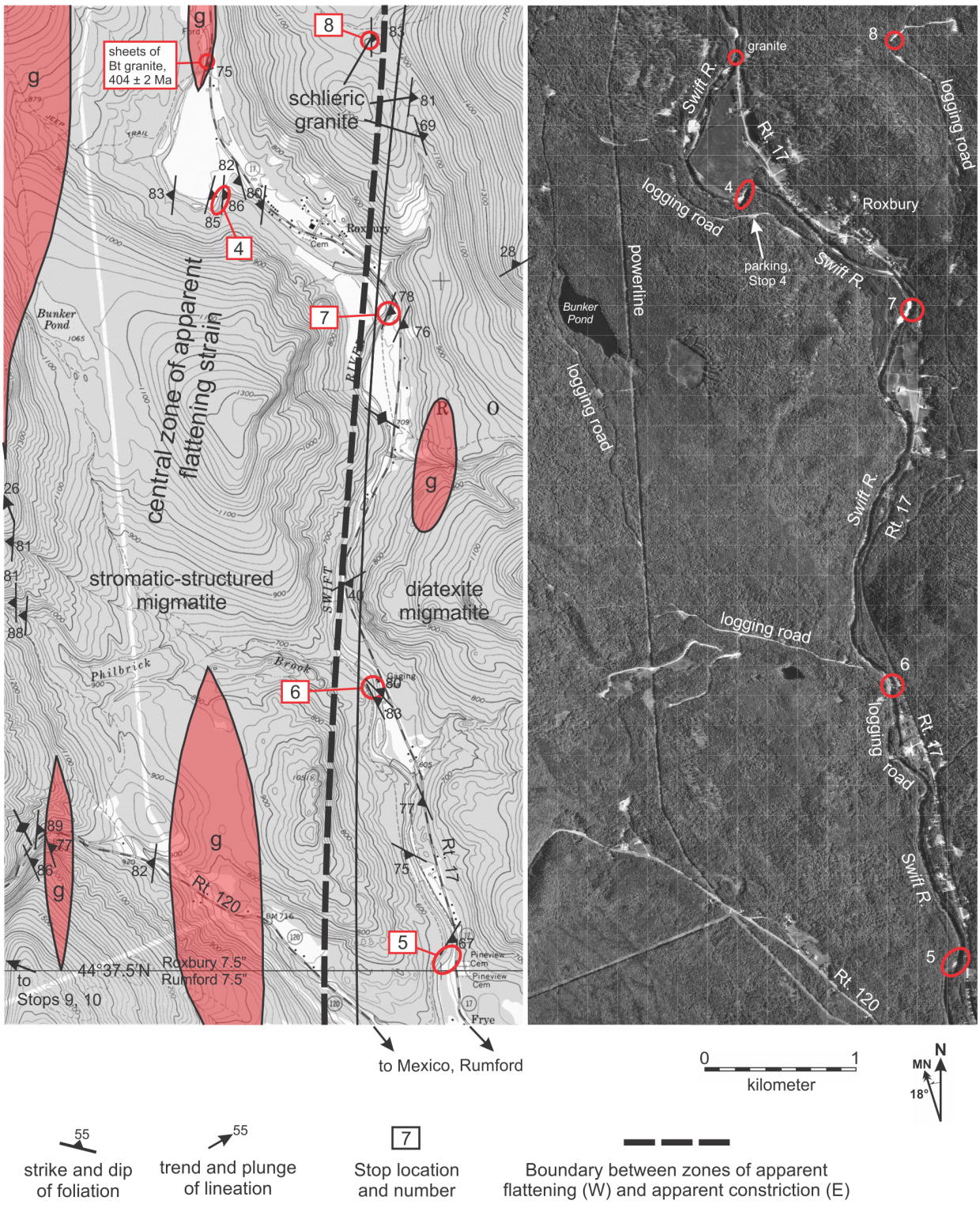

Figure 13. Topographic, aerial and locations maps with simplified geology for the area of STOPS 4 through 8. Structural data are taken from Solar (1999). Age of the Bt granite from Solar et al. (1998). Symbols are consistent with those on Figs. 2 and 11; g is granite. See the road log for details of STOP locations/geology.

26.7 Park in clearing on right (Figure 13). Walk across the road and walk into the woods towards the Swift River. You will find a trail before reaching the river. Follow this trail to the right. There are two outcrops for this stop, a steep portion almost immediately accessible after finding the trail, and an outcrop of stream pavement farther along the trail, just before the right-hand curve in the river and trail.

STOP 4: STROMATIC-STRUCTURED METATEXITE MIGMATITE AND SUB-CONCORDANT METER-SCALE LEUCOGRANITE SHEETS, SWIFT RIVER, ROXBURY, MAINE
(UTM 4947726N, 373045W)

See Figure 13 for location. Stromatic-structured metatexite migmatite formed during plastic deformation of metasedimentary rock. Locally, alternating layers of pelite and psammite similar to that in the non-migmatite stratigraphic succession are apparent, to suggest the protolith of the metatexite migmatite was rocks similar to the Rangeley stratigraphic sequence. Mica foliation, leucosomes and melt-depleted host rock domains [interpretation based on geochemical data shown in Figure 9 and discussed in Solar and Brown (2001b)] are all sub-parallel, all steeply E-dipping. Granite sheets are concordant to sub-concordant, and display no record of internal plastic strain, but are pinched-and-swelled to suggest deformation in the host rock continued after intrusion. The sheets have a biotite foliation parallel to the structure of the sheets. This rock is within the central zone of apparent flattening strain (Figures 2, 3 and 13), along strike from Coos Canyon (STOP 1; Figure 11). The thickest granite sheet yielded a concordant U-Pb zircon crystallization age of 408 ± 2 Ma (Solar et al., 1998). Granite-migmatite relations in the steep (south) part of the outcrop suggest that progressive sheeting of granite constructed kilometer-scale lens-shaped plutons in the migmatite domain (see Figures 2, 3 and 13). Local outcrops are meter-scale granite sheets only, consistent with this interpretation (see Figure 13, top for example location). The outcrop of stream pavement was mapped at the 1:24 scale by Chmura (2001).

Mileage

26.7 Return to vehicles and return to Rt. 17.
33.0 Turn left to go north toward Roxbury (Figure 13). Look for Pineview Cemetery on the right.
33.3 Pull over on the right and park just north (past) of the cemetery. The outcrops for STOP 5 are in the Swift River across the street (west of Rt. 17, Figure 13). Descend down the steep grade from the road to the stream pavement.

STOP 5: DIATEXITE (HETEROGENEOUS) MIGMATITE AND SUB-CONCORDANT CENTIMETER-SCALE LEUCOGRANITE CYLINDERS, SWIFT RIVER, SOUTH OF ROXBURY (FRYE), MAINE
(UTM 4942666N, 374467W)

See Figure 13 for location. The diatexite migmatite is residual in composition similar to that of the stromatic-structured migmatite (STOP 4), but in contrast, leucosome structures are generally rod-shaped in the diatexite migmatite with long dimensions plunging steeply E, similar to the mineral fabric. This rock is typical of all rocks in the northern TAD where it is within a zone of apparent constrictional strain (Figure 2; Solar and Brown, 2001a, 2001b). West-dipping surfaces display leucosome rod-shapes end-on (cross section), whereas steeply south-dipping surfaces are sub-parallel to the long dimension.

Mileage

33.3 Continue north on Rt. 17 toward Roxbury.
34.6 Park on the right side of the road (opposite side of the road from the river) just across from a private dirt parking lot located along pavement outcrops in Swift River. The outcrops for STOP 6 are in the river here, but there is an outcrop for this stop on the east side of the road.

STOP 6: DIATEXITE (HETEROGENEOUS) MIGMATITE, THREE-POOLS (A.K.A. SWIFT RIVER FALLS), SWIFT RIVER, SOUTH OF ROXBURY, MAINE (UTM 4945237N, 374010W)

See Figure 13 for location. Diatexite migmatite that is residual in composition [interpretation based on geochemical data shown in Figure 8 and discussed in Solar and Brown (2001b)] similar to that of STOP 5.

Again, leucosome structures are generally rod-shaped with long dimensions plunging steeply E similar to the mineral fabric. This rock is within the west margin of the intervening zone between the two limbs of the central zone of apparent flattening strain. The outcrop in the River is transitional to stromatic-structured metatexite migmatite located to the west (just across the river in the woods; Figure 13) and homogeneous diatexite migmatite located on the east side of Rt. 17 (poorly exposed across from the parking lot). The diatexite migmatite on the east side of Rt. 17 is typical of all rocks in the northern TAD within the intervening zone of apparent constrictional strain (Figure 2; Solar and Brown, 2001a, 2001b).

Mileage

34.6 Continue north toward Roxbury (Figure 13).
36.3 At just before the antique shop at the south end of Roxbury town, pull over on the left carefully where the Swift River returns to the roadside, at a metal gate on a dirt road that follows the river (or pass the gate and turn around and park at the gate). The outcrop for STOP 7 is in the river. Take note that access to the river outcrop is via private property.

STOP 7: DIATEXITE (HETEROGENEOUS) MIGMATITE AND SUB-CONCORDANT METER-SCALE CYLINDERS OF LEUCOGRANITE, SWIFT RIVER, ROXBURY, MAINE (UTM 4946963N, 374154W)

See Figure 13 for location. Meter-scale cylindrical granite bodies within diatexite migmatite. The diatexite migmatite is residual in composition (interpretation based on geochemical data discussed in Solar and Brown, 2001b) suggesting melt extraction. A meter-scale residual block of diatexite just north of center of the exposure is the "block of Bt-Grt schist" of Figure 8 and is taken to represent extreme melt depletion in the migmatite domain. Meter-scale structures are pipe-shaped with their long dimensions plunging steeply E similar to the mineral fabric. This rock is within the intervening zone between the two limbs of the central zone of apparent flattening. Brown and Solar (1999) suggest the cylinders represent transfer structures for melt that supplied plutons above (Solar and Brown, 2001b). The outcrop is mapped at 1:24 scale (Chmura, 2001).

Mileage

36.3 Return south on Rt. 17 (south of Roxbury town).
36.6 Turn left onto a dirt logging road (Figure 13) called locally "Walker Brook Rd.", and head uphill into the woods on the east side of Rt. 17. Please exercise caution on this road; it is active.
36.7 Turn left at the intersection to go north on a logging road (Figure 13).
38.3 At just after a sharp right turn, pull over at the pavement outcrop along the right side (Figure 13).

STOP 8: SCHLIERIC GRANITE IN THE TRANSITION ZONE BETWEEN STROMATIC-STRUCTURED METATEXITE MIGMATITE AND DIATEXITE MIGMATITE, NORTHEAST OF ROXBURY, MAINE (UTM 4948786N, 374079W)

See Figure 13 for location. Cumulate granite with a penetrative steeply E dipping schlieric fabric. The fabric is concordant with the stromatic migmatite structure, but this rock is located within the transition zone between stromatic migmatite to the west (downhill) and diatexite to the east (uphill) (Solar and Brown, 2001b). This rock includes schollen of calc-silicate rich metasedimentary rock that have apparently boudinaged and rotated during what was probably en masse melt-accommodated granular flow of this crystal-rich magma. See Figure 8 for geochemical data from rocks from this outcrop.

Mileage

38.3 Return back to Rt. 17.
40.0 Turn left on Rt. 17 to go south.
42.8 Turn right onto the access road for Rt. 120.
43.0 Pass intersection with dirt logging road to STOP 4.
43.1 Right turn to go west on Rt. 120.
48.6 Intersection of Rt. 120 and Roxbury Notch Road.
50.1 Ellis River outcrops of granite of the Mooselookmeguntic Igneous Complex.

50.4 Black Brook.
51.9 Right turn at T-intersection to continue on Rt. 120.
52.1 Turn right (north) onto S. Arm Road.
54.5 Bridge over Black Brook and intersection with Lohnes Road on right.
54.9 Outcrop of aplite of the Mooselookmeguntic Igneous Complex.
56.6 Turn left onto dirt road and drive down 0.1 miles to Black Brook and STOP 9.

STOP 9: TWO-MICA GRANITE OF THE SOUTHERN MOOSELOOKMEGUNTIC IGNEOUS COMPLEX (MIC), BLACK BROOK ALONG SOUTH ARM RD. AT "SILVER RIPPLE CASCADE," ANDOVER SURPLUS, MAINE (UTM 4949556N, 362070W)

Medium- to coarse-grained Bt granodiorite (local quartz) in ~1-10m blocks in fine-grained Bt granite that is typical of the southern lobe of the MIC. This stop is "96-60" of Tomascak et al. (2005). Magmatic Bt foliation in the granite is steeply dipping, and pegmatite dikes cut both types of rocks. Whole rock geochemistry and age data from this location are discussed in Tomascak et al. (2005).

Mileage

56.7 Return to S. Arm Road, and turn right to backtrack to Rt. 120.
61.4 Turn right onto Rt. 120 and continue to the town of Andover.
61.9 Continue straight through the intersection with Rt. 5 in the Andover town center.
63.6 Intersection with Right Cross Road (or Cross St.). Rocks of Stop 10 are in the stream below the bridge.

STOP 10. MONZODIORITE OF THE MOOSELOOKMEGUNTIC IGNEOUS COMPLEX, ANDOVER, MAINE (UTM 4925999N, 357943W)

Medium-grained Bt granodiorite with a weak N-S foliation and schlieren typical of the western part of the MIC. This stop is "J98-40" of Tomascak et al. (2005). This granodiorite is not as coarsely foliated as similar rocks at STOP 9 (in the blocks). Whole rock geochemistry and age data from this location are discussed in Tomascak et al. (2005).

END OF TRIP.

Bethel, Maine is approximately 30-35 minutes drive time From STOP 10. Backtrack to Andover and turn right at the intersection to follow Rt. 5 to Rt. 2. Turn right on Rt. 2. Bethel is 13 miles from that point.

ACKNOWLEDGEMENTS

We are pleased to offer this trip as part of the 2017 NEIGC and we thank the coordinators for asking us to participate. The leaders are grateful to Chuck Guidotti and E-an Zen for getting us started in the Rangeley-Rumford area. We thank all those who have helped us during the course of the work that has produced the data and interpretations presented as this guide. Misconceptions and errors are our own. We remain grateful for the field support of Fred and Cheryl England formerly of Weld, ME, Anna Solar, and Heather McCarthy. We are thankful for partial support of this work from the NSF (EAR-9705858), the GSA Research Grants Program, the Department of Geology, University of Maryland, the Department of Earth Sciences, SUNY College at Buffalo, and the Department of Atmospheric and Geological Sciences, SUNY Oswego.

REFERENCES CITED

Arth, J.G., and Ayuso, R.A., 1997, The Northeast Kingdom batholith, Vermont: Geochronology and Nd, O, Pb, Sr isotopic constraints on the origin of Acadian granitic rocks. In: Sinha, A.K., Whalen, J.B., Hogan, J.P. (Eds.), The Nature of Magmatism in the Appalachian Orogen: Geological Society of America Memoir 191, p. 1-17.

Ayuso, R.A., and Schulz, K.J., 2003, Nd-Pb-Sr isotope geochemistry and origin of the Ordovician Bald Mountain and Mount Chase massive sulfide deposits, northern Maine: In: Goodfellow, W.D. (Ed.), Volcanogenic massive sulfide deposits of the Bathurst district in northern Maine. Economic Geology Monograph 11.

Berry, H.N., IV, and Hussey, A.M., II, 1998, Bedrock geology of the Portland 1:100,000 quadrangle, Maine and New Hampshire: Maine Geological Survey Open File Report No. 98-1.

Bradley, D.C., Tucker, R.D., Lux, D.R., Harris, A.G., and McGregor, D.C., 1998, Migration of the Acadian orogen and foreland basin across the northern Appalachians: U.S. Geological Survey, Open-File Report 98-770, 79 p.

Brown, M., and Solar, G.S., 1998a, Shear zone systems and melts: feedback relations and self organization in orogenic belts: Journal of Structural Geology, v.20, p. 211-227.

Brown, M., and Solar, G.S., 1998b, Granite ascent and emplacement during contractional deformation in convergent orogens: Journal of Structural Geology, v.20, p. 1365-1393.

Brown, M., and Solar, G.S., 1999, The mechanism of ascent and emplacement of granite magma during transpression: a syntectonic granite paradigm: Tectonophysics, v.312, p. 1-33.

Chmura, S.M., 2001, Comparative detailed mapping of contrasting types of migmatites, Central Maine belt, Roxbury area, western Maine: unpublished undergraduate Honors thesis, State University of New York, College at Buffalo, 90 p.

Creasy, J.W., and Robinson, A.C., 1997, Bedrock geology of the Gray 7.5 minute quadrangle, Cumberland County, Maine: Maine Geological Survey Open File Report No. 97-3.

Dias, R., and Ribeiro, A., 1994, Constriction in a transpressive regime: an example in the Iberian branch of the Ibero-Armorican arc: Journal of Structural Geology, v.16, p. 1543-1554.

Guidotti, C.V., 1970, The mineralogy and petrology of the transition from lower to upper sillimanite zone in the Oquossoc area, Maine: Journal of Petrology, v.11, p. 277-336.

Guidotti, C.V., 1974, Transition from staurolite to sillimanite zone, Rangeley quadrangle, Maine: Geological Society of America Bulletin, v.85, p. 475-490.

Guidotti, C.V., 1989, Metamorphism in Maine: an overview: In: Studies in Maine Geology, v.3, p. 1-19.

Guidotti, C.V., 2000, The classic high-T – low-P metamorphism of west-central Maine, USA: Is it post-tectonic or syn-tectonic? Evidence from porphyroblast-matrix relations – Discussion: Canadian Mineralogist, Kretz Volume, v.38, p. 995-1006.

Hatch, N.L., Jr., Moench, R.H., and Lyon, J.B., 1983, Silurian-lower Devonian stratigraphy of eastern and south-central New Hampshire: Extensions from western Maine: American Journal of Science, v.283, p. 739-761.

Holdaway, M.J., Guidotti, C.V., Novak, J.M., and Henry, W.E., 1982, Polymetamorphism in medium- to high-grade pelitic metamorphic rocks, west-central Maine: Geological Society of America Bulletin, v.93, p. 572-584.

Holdaway, M.J., Mukhapodhyay, B., Dyar, M.D., Guidotti, C.V., and Dutrow, B.L., 1997, Garnet-biotite geothermometry revised: new Margules parameters and a natural specimen data set from Maine: American Mineralogist, v.82, p. 582-595.

Johnson, T.E., Brown, M., and Solar, G.S., 2003, Low-pressure subsolidus and suprasolidus phase equilibria in the MnNCKFMASH system. Constraints on conditions of regional metamorphism in western Maine, northern Appalachians: American Mineralogist, v.88, p. 624-638.

Moench, R.H., 1970, Premetamorphic down-to-basin faulting, folding, and tectonic dewatering, Rangeley area, western Maine: Geological Society of America Bulletin, v.81, p. 1463-1496.

Moench, R.H., and Boudette, E.L., 1970, Stratigraphy of the northwest limb of the Merrimack synclinorium in the Kennebago Lake, Rangeley, and Phillips quadrangles, western Maine: Guidebook for Field Trips in the Rangeley Lakes - Dead River Region, Western Maine, New England Intercollegiate Geological Conference, 62nd Annual Meeting, p. A:1-25.

Moench, R.H., Boone, G.M., Bothner, W.A., Boudette, E.L., Hatch, N.L., Jr., Hussey, A.M., II, Marvinney, R.G., and Aleinikoff, J.N., 1995, Geologic map of the Sherbrooke-Lewiston area, Maine, New Hampshire, and Vermont, United States, and Quebec Canada: U.S. Geological Survey Map I-1898-D, scale 1:250,000.

Moench, R.H., and Aleinikoff, J.N., 2002, Stratigraphy, geochronology, and accretionary terrane settings of two Bronson Hill arc sequences, northern New England: Physics and Chemistry of the Earth, v.27, p. 47-95.

Patiño Douce, A.E., and Harris, N., 1998, Experimental constraints on Himalayan anatexis: Journal of Petrology, v.39, p. 689-710.

Pressley, R.A., and Brown, M., 1999, The Phillips pluton, Maine, USA: evidence for heterogeneous crustal sources for granite ascent and emplacement mechanisms in convergent orogens: Lithos, v.49, p. 335-366.

Robin, P.–Y.F., and Cruden, A.R., 1994, Strain and vorticity patterns in ideally ductile transpression zones: Journal of Structural Geology, v.16, p. 447-467.

Sawyer, E.W., 2008, Atlas of Migmatites: The Canadian Mineralogist Special Publication 9, Mineralogical Association of Canada, NRC Research Press, 371p.

Solar, G.S., 1999, Structural and petrological investigations in the Central Maine belt, west-central Maine, with special reference to the migmatites: unpublished Ph.D. dissertation, University of Maryland, 364 p.

Solar, G.S., and Brown, M., 1999, The classic high-T – low-P metamorphism of west-central Maine, USA: Is it post-tectonic or syn-tectonic? Evidence from porphyroblast-matrix relations: Canadian Mineralogist, Kretz Volume, v.37, p. 311-333.

Solar, G.S., and Brown, M., 2000, The classic high-T – low-P metamorphism of west-central Maine, USA: Is it post-tectonic or syn-tectonic? Evidence from porphyroblast-matrix relations – Reply: Canadian Mineralogist, v.38, p. 1007-1026.

Solar, G.S., and Brown, M., 2001a, Deformation partitioning during transpression in response to Early Devonian oblique convergence, northern Appalachian orogen, USA: Journal of Structural Geology, v.22**,** p. 1043-1065.

Solar, G.S., and Brown, M., 2001b, Petrogenesis of Migmatites in Maine, USA: Possible Source of Peraluminous Granite in Plutons: Journal of Petrology, v.42, p. 789-823.

Solar, G.S., Brown, M., and Tomascak, P.B., 2001, Deformation, metamorphism, and granite ascent in western Maine: In West, D.P. and Bailey, R.H. (Eds.), Guidebook for Geological Field Trips in New England, 2001 Annual Meeting of the Geological Society of America, Boston, MA, Trip Q, 30 p.

Solar, G.S., Pressley, R.A., Brown, M., and Tucker, R.D., 1998, Granite ascent in convergent orogenic belts: Testing a model: Geology, v.26, p. 711-714.

Solar, G.S., and Tomascak, P.B., 2001, Is there a relation between transpressive deformation and pluton emplacement in southern Maine?: Geological Society of America, Abstracts with Programs, v.33.

Steely, C., 2001, The origin and significance of porphyroblast-matrix fabric obliquities, Coos Canyon, Maine: unpublished undergraduate thesis, University of Maryland, 50 p.

Thompson, A.B., and Tracy, R.J., 1976, Model systems for anatexis of pelitic rocks. II, facies series melting and reaction in the system CaO – $KAlO_2$ – $NaAlO_2$ – Al_2O_3 – SiO_2 – H_2O: Contributions to Mineralogy and Petrology, v.70, p. 429-438.

Tomascak, P.B., Krogstad, E.J., and Walker, R.J., 1996a, U-Pb monazite geochronolgy of granitic rocks from Maine:implications for late Paleozoic tectonics in the northern Appalachians: Journal of Geology, v.104, p. 185-195.

Tomascak, P.B., Krogstad, E.J., and Walker, R.J., 1996b, Nature of the crust in Maine, USA: evidence from the Sebago batholith: Contributions to Mineralogy and Petrology, v.125, p. 45-59.

Tomascak, P.B., Brown, M., Solar, G.S., Becker, H.J., Centorbi, T.L., and Tian, J., 2005, Source contributions to Devonian granite magmatism near the Laurentian border, New Hampshire and western Maine, USA: Lithos, v.80, p. 75-99.

van Staal, C.R. and de Roo, J.A., 1995, Mid-Paleozoic tectonic evolution of the Appalachian Central Mobile Belt in northern New Brunswick, Canada: collision, extensional collapse and dextral transpression: In Hibbard, J.P., van Staal, C.R., and Cawood, P.A. (Eds.), Current Perspectives in the Appalachian-Caledonian Orogen, Geological Association of Canada Special Paper 41, p. 367-389.

van, Staal, C.R., Dewey, J.F., MacNiocaill, C., and McKerrow, W.S., 1998, The Cambrian-Silurian tectonic evolution of the northern Appalachians and British Caledonides: History of a complex, west and southwest Pacific-type segment of Iapetus: Geological Society Special Publication.

West, D.P., Jr., 1999, Timing of displacements along the Norumbega fault system, south-central and south-coastal Maine: In Ludman, A. and West, D.P., Jr. (Eds.), Norumbega Fault System of the Northern Appalachians, Geological Society of America Special Paper 331, p. 167-178.

West, D.P., Jr. and Hubbard, M.S., 1997, Progressive localization of deformation during exhumation of a major strike-slip shear zone: Norumbega fault zone, south-central Maine: Tectonophysics, v.273, p. 185-202.

Whalen, J.B., Roger, N., van Staal, C.R., Longstaffe, F.J., Jenner, G.A., and Winchester, J.A., 1998, Geochemical and isotopic (Nd, O) data for Ordovician felsic plutonic and volcanic rocks of the Miramichi Highlands: petrogenetic and metallogenic implications for the Bathurst Mining Camp: Canadian Journal of Earth Sciences, v.35, p. 237-252.

Whalen, J.B., Fyffe, L.R., Longstaffe, F.J., and Jenner, G.A., 1996, The position of the Gander-Avalon boundary, southern New Brunswick, based on geochemical and isotopic data from granitoid rocks: Canadian Journal of Earth Sciences, v.33, p. 129-139.